

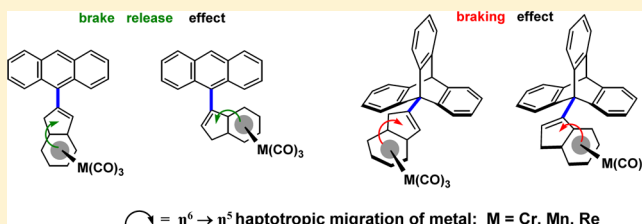
High and Low Rotational Barriers in Metal Tricarbonyl Complexes of 2- and 3-Indenyl Anthracenes and Triptycenes: Rational Design of Molecular Brakes

Kirill Nikitin,* Cornelia Bothe, Helge Müller-Bunz, Yannick Ortin, and Michael J. McGlinchey*

School of Chemistry & Chemical Biology, University College Dublin, Belfield, Dublin 4, Ireland

Supporting Information

ABSTRACT: Syntheses and X-ray crystal structures are reported for a series of $M(\text{CO})_3$ derivatives ($M = \text{Cr}, \text{Re}$) of phenyl and also 2- and 3-indenyl anthracenes and triptycenes. In each case, the rotational barrier about the bond linking the two organic fragments was evaluated both experimentally by VT or 2D-EXSY NMR and by calculation at the DFT level. Attachment of the metal tripod to the indenyl moiety in an η^6 fashion does not markedly change the barrier relative to that for the free ligand but lowers the symmetry so as to facilitate its direct measurement. Interestingly, an $\eta^6 \rightarrow \eta^5$ haptotropic shift of the $\text{Cr}(\text{CO})_3$ moiety in 9-indenylanthracenes led to a somewhat lowered barrier, probably attributable to an increase in the ground state energy rather than to decreased steric interactions in the transition state. In contrast, in indenyltriptycenes $\eta^6 \rightarrow \eta^5$ migration of the $M(\text{CO})_3$ unit along the indenyl skeleton and closer to a paddlewheel leads to a very significant increase in the rotational barrier. These effects can be rationalized in terms of angular steric strain and multiple interactions in the ground state and in the transition state. The results not only provide semiquantitative data on the steric effects of η^6 -phenyl and η^6 - or η^5 -indenyl $M(\text{CO})_3$ fragments but are also discussed with relevance to their role in organometallic molecular brakes.



INTRODUCTION

Mechanical systems, and their molecular analogues, exhibit two fundamental kinds of motion: translation and/or rotation. All currently known examples of controlled or random intramolecular mechanical motion may be categorized as either translational (shuttles) or rotational (rotors).¹ The past decade has been graced by a plethora of reports describing the design and function of molecular machines employing either rotation or translation.^{2,3} However, molecular systems explicitly combining both types of intramolecular motion are less commonly described.

In our recent study of the dynamic behavior of [$\{(\eta^6\text{-}2\text{-(9-triptycyl)indene}\}\text{Cr}(\text{CO})_3\}$] (**1**), we demonstrated how the rotor–shuttle concept can work in such a controlled molecular motion system, whereby the sliding movement of a metal carbonyl tripod severely hinders the rotation of a triptycene moiety (Scheme 1). For the first time, a directed suprafacial migration was combined with the rotational motion of a molecular paddlewheel in a compact molecular design.⁴ The transition from an η^6 to an η^5 structure, **1** \rightarrow **2**, is accompanied by an increase of the rotational barrier by $\sim 12 \text{ kcal mol}^{-1}$, corresponding at ambient temperature to a 10^8 -fold rate decrease.

While the observed molecular braking effect can apparently be viewed as a simple consequence of “jamming” of the triptycene blades by a carbonyl of the $\text{Cr}(\text{CO})_3$ tripod, a more detailed understanding of this phenomenon requires theoretical and experimental comparative analysis of the structures and

dynamic behavior of a series of related organic and organometallic structures. Recent studies^{5,6} of the rigid rotational systems **3–8** clearly demonstrated that the very substantial rotational barriers in the anthracenes **3b** and **5** arise from unavoidable steric clashes of hydrogens in the indenyl or phenyl ring with the peri positions of the anthracene fragment (Chart 1). In contrast to the situation in the anthracenes **3b** and **5**, the corresponding triptycenes **4b** and **6** can access an energetically more favorable conformation whereby the planar indenyl or phenyl moiety can bend away from the 3-fold axis of the triptycene and slide partially into the valley between the blades, thus alleviating the steric strain and reducing the rotational barrier. However, further comparison with the analogous ferrocenylanthracene and -triptycene **7** and **8**, respectively, suggests that the presence of the additional unsubstituted free-rotating (η^5 -cyclopentadienyl)iron fragment *inverts* the situation once again, now making the rotation of the nominally C_3 -symmetrical triptycene paddlewheel in **8** *slower* than that of the flat anthracene moiety in **7**.⁶

Although rotational barriers arising in the molecules containing planar anthracenyl or paddlewheel-shaped triptycyl fragments directly connected to an aromatic moiety bearing an *orthogonally attached* organometallic group remain largely unexplored, there is particular relevance to the structures and dynamics of organometallic atropisomers. Thus, axially chiral

Received: June 8, 2012

Published: August 22, 2012

Scheme 1. Illustration of a Rotor–Shuttle Controlled Molecular Motion System

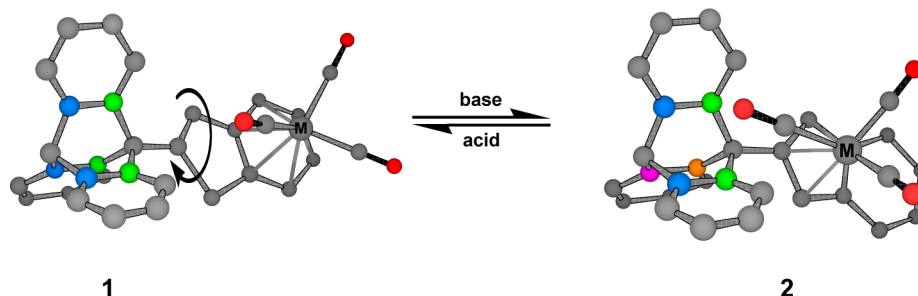
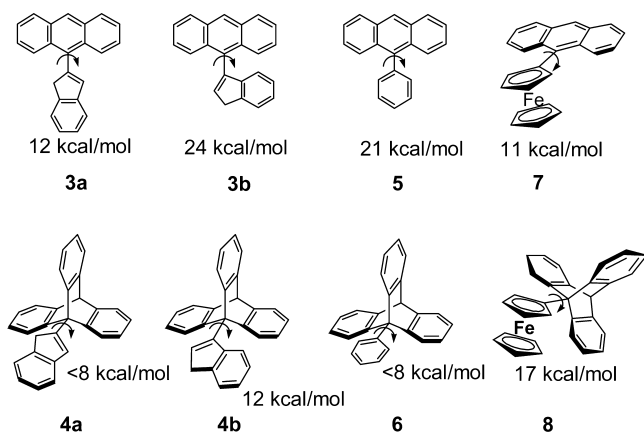
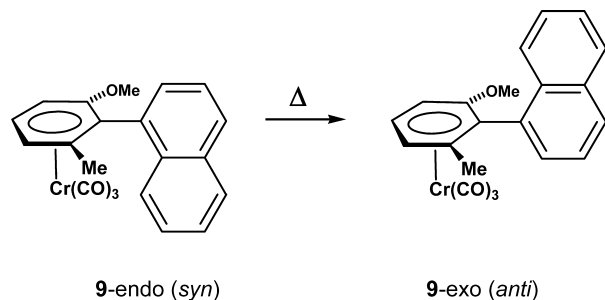


Chart 1. Intramolecular Rotation Barriers in the Anthracenes 3, 5, and 7 and Triptycenes 4, 6, and 8



biaryls, made by palladium-catalyzed cross-couplings, can lead to atropisomeric mixtures.⁷ Typically, as illustrated in Scheme 2, the initially formed naphthyl-substituted arene-Cr(CO)₃

Scheme 2. Rotation about the Single Bond Linking the Phenyl and Naphthyl Fragments in 9, Bringing about Diastereomerization of Chiral Atropisomers



complex **9-syn** undergoes axial rotation to furnish its thermodynamically favored diastereomer **9-anti**, when heated in a high-boiling solvent.⁸ This phenomenon has been exploited in the syntheses of natural products such as the alkaloids Korupensamine A and B.⁹

Herein we report the syntheses, crystal structures, theoretical modeling, and dynamic NMR behavior of a series of closely related π -arene complexes containing tripodal M(CO)₃ moieties, where M is chromium or rhenium. We show that such organometallic fragments clearly evoke unusual additional steric interactions and strongly influence the rotational barriers. Moreover, they provide versatile internal molecular labels that lower the molecular symmetry and engender very substantial

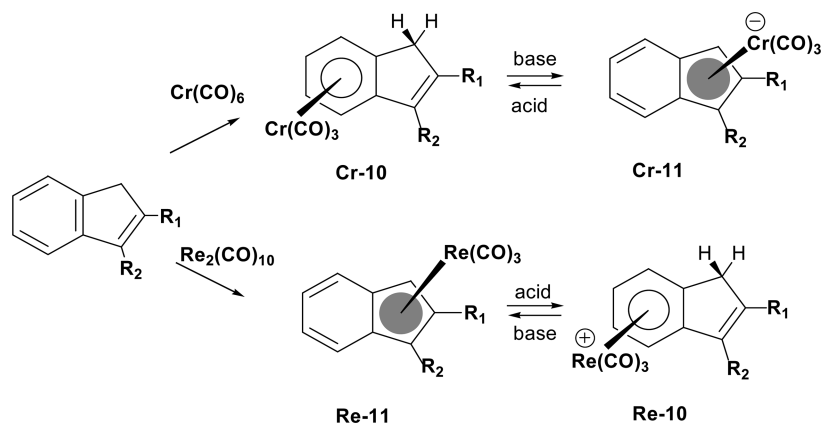
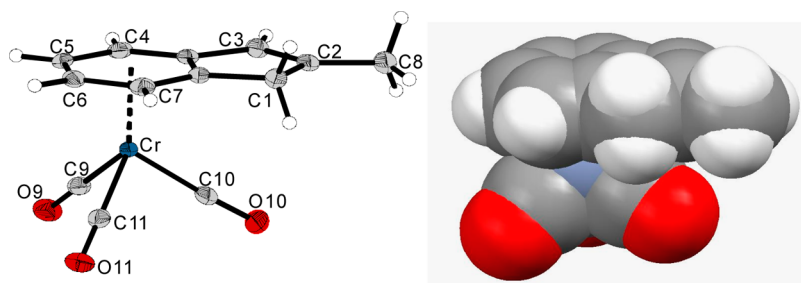
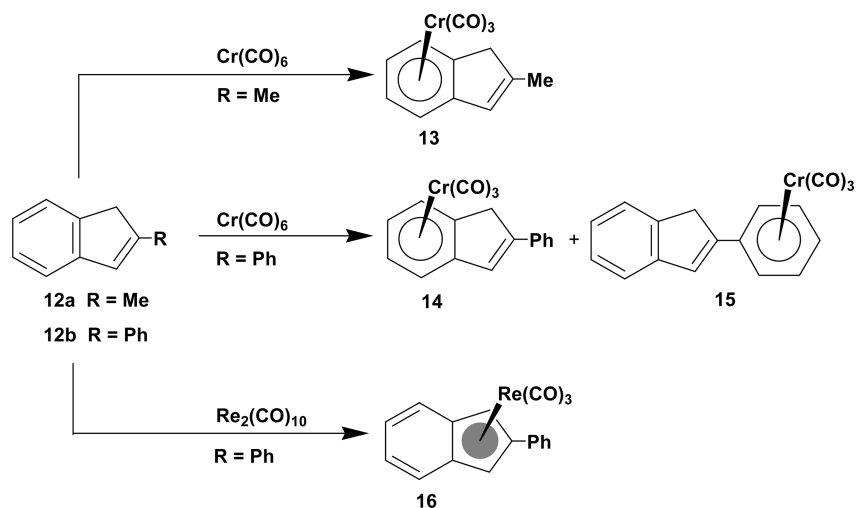
diamagnetic anisotropy,^{6,10} both helping to observe and quantify the rotational barriers. Finally, since the site of attachment of the tricarbonylchromium group can be altered by applying a chemical stimulus, some of the systems described also have an in-built molecular shuttle function.

Because the archetypal haptotropic molecular brake **1** can be viewed as the juxtaposition of a paddlewheel and an indene or indenyl moiety bearing a metal tricarbonyl group, the present study focuses on chromium and rhenium tricarbonyl derivatives of hydrocarbons containing an indene/indenyl fragment and/or a C₃-symmetrical paddlewheel-shaped triptycene rotor.

RESULTS AND DISCUSSION

Our continuing interest in the indene scaffold is primarily driven by the fact that an organometallic moiety such as Cr(CO)₃, [Mn(CO)₃]⁺, or [Rh(C₂H₄)₂]⁺ can be attached to the six-membered aromatic ring of an indene (as in the η^6 complex Cr-**10**, Scheme 3). However, upon deprotonation by a strong base, the organometallic unit undergoes a suprafacial migration driven by its ability to delocalize the negative charge on the five-membered ring of the indenide anion, typically leading to the anionic η^5 complex Cr-**11**.¹¹ On the other hand, an isolobal [Re(CO)₃]⁺ moiety can be attached to the five-membered ring of the indenide anion (as the η^5 complex Re-**11**, Scheme 3). Such relatively robust molecules are excellent models for structural and dynamic studies of the isolobal anionic chromium derivatives Cr-**11**. Moreover, under appropriate protonation conditions, a neutral complex typified by Re-**11** or (η^5 -indenyl)Rh(C₂H₄)₂ can undergo the reverse sliding movement, thus forming a cationic η^6 complex, as in Re-**10**.¹¹

Let us consider a C₃-symmetrical triptycyl rotor connected to a flat aromatic fragment, exemplified by phenyl or indenyl as in Chart 1, in which the 3-fold symmetry of the triptycene is broken and two of the blades are no longer equivalent to the third one. This nonequivalence, at least in principle, can be observed and used for the determination of the rotational barrier.⁵ However, analysis of dynamic 500 MHz ¹H NMR data demonstrated that rotation in both 9-(2-indenyl)triptycene and 9-phenyltriptycene (**4a** and **6**, respectively), is fast on the NMR time scale at 193 K, and the rotational barrier is less than ~9 kcal mol⁻¹. In this context, we note that the much slower internal rotation in 9-(3-indenyl)anthracene (**3b**) and 9-phenylanthracene (**5**) cannot be directly observed, as the terminal benzo rings (blades) of the anthracene remain equivalent, owing to their dynamic symmetry. However, judicious lowering of their time-averaged C_{2v} symmetry, as in 9,10-bis(*m*-fluorophenyl)anthracene or 9-naphthyl-10-phenylanthracene, revealed the phenyl rotation barrier to be in excess of 20 kcal mol⁻¹.^{5c}

Scheme 3. Relationships between η^5 - and η^6 -Indene Metal Carbonyl ComplexesScheme 4. Preparation of η^6 -Cr(CO)₃ and η^5 -Re(CO)₃ Complexes from the Indenes 12a,bFigure 1. Molecular structure of the η^6 complex 13. The space-filling representation shows that no close contacts are evident.

One can anticipate that further modification of the indenyl or phenyl substituent in molecules 3–6 by incorporation of a metal tricarbonyl moiety should lower the molecular symmetry such that internal rotation in the anthracenes 3 and 5, and also in the triptycenes 4 and 6, may be conveniently observed by NMR spectroscopy. Accordingly, we have prepared and studied the dynamic behavior of a series of organometallic derivatives of these and other closely related hydrocarbon scaffolds. Inspired by a theoretically predicted,¹² and very recently experimentally verified,^{5e} high rotational barrier in 9-phenylanthracene (5), the rotational energy profiles of these new organometallic systems have been simulated by calculations at the DFT level. Gratifyingly, the theoretical studies are in reasonable agreement with the experimentally observed trends.

Internal Rotation in Metal Carbonyl Derivatives of 2-Methyl- and 2-Phenylindenes. As shown in Scheme 3, substituted indenes react readily with appropriate metal carbonyls at elevated temperature, thus yielding complexes such as Cr-10 and Re-11.¹³ While treatment with rhenium carbonyl leads selectively to η^5 complexes, reactions with Cr(CO)₆ furnish a mixture of several possible metalated derivatives when multiple aromatic fragments are present as substituents R₁ and R₂.¹⁴

Typically, when 2-methylindene (12a) was heated with Cr(CO)₆ in 1,4-dioxane, only the η^6 complex 13 was formed (Scheme 4). The molecular structure of 13, shown in Figure 1, clearly suggests that, as the methyl group does not engage in steric clashes with the rest of the molecule, the methyl

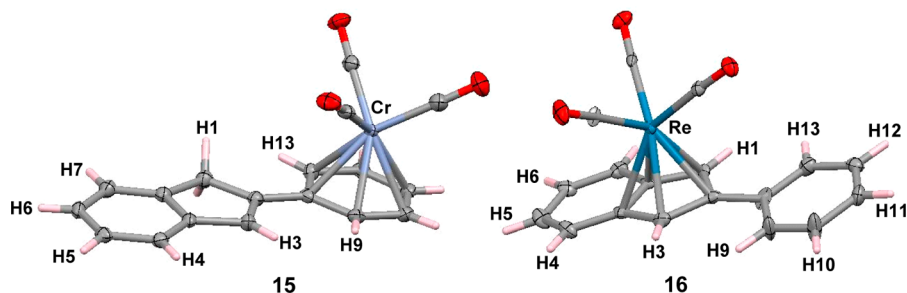
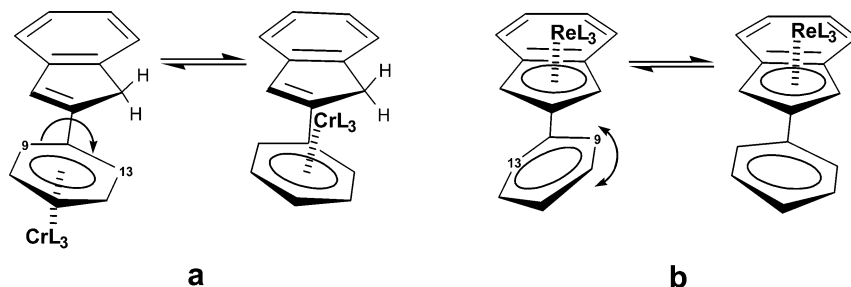


Figure 2. Molecular structures of (a) $[\eta^6\text{-(2-indenyl)benzene}]$ tricarbonylchromium(0) (**15**) and (b) $[\eta^5\text{-(2-phenyl)indenyl}]$ tricarbonylrhenium(I) (**16**).

Scheme 5. (a) Minimum 90° Flip of the Indenyl Ring Relative to the $(\text{phenyl})\text{Cr}(\text{CO})_3$ Fragment Required to Equilibrate the C(9) and C(13) Positions and the Methylene Hydrogens in **15** and (b) Achievement of Such Equivalence in **16** by Just a Minor Oscillation of the Phenyl Ring Relative to the Indenyl Plane



rotational barrier should be low.^{11d,15} Indeed, as revealed by X-ray crystallography, the methyl group is rotationally disordered in the solid state.

In contrast, the reaction of 2-phenylindene (**12b**) with chromium hexacarbonyl yielded two isomeric products: in the η^6 complex **14**, ^1H and ^{13}C NMR data indicated that the chromium was positioned on the six-membered ring of the indene, while in **15** the chromium was η^6 -bonded to the phenyl ring. Unfortunately, this 1/2 mixture could not be conveniently separated on a preparative scale, but slow crystallization furnished X-ray-quality crystals of **15**, and Figure 2a shows that the dihedral angle between the phenyl ring and the indenyl framework is only 2° . Interestingly, even in this essentially coplanar conformation the closest distance between the two spatially adjacent hydrogens H(3) and H(9) is a very comfortable 2.24 Å, (sum of vdW radii 2.05 Å).¹⁶ Moreover, a DFT study of this molecular system revealed that a full 180° rotation of the phenyl (Scheme 5a) would evoke a potential barrier not exceeding 6 kcal mol⁻¹.

Turning now to $(\eta^5\text{-2-phenylindenyl})\text{Re}(\text{CO})_3$ (**16**), which can be efficiently prepared in 70% yield by transmetalation of 2-phenyl-1-trimethylstannyindene (but, perhaps, more conveniently by direct metalation of **12b**, as described in the Experimental Section), one can see from Figure 2b that the phenyl substituent is no longer coplanar with the indenyl ring. The dihedral angle ranges from 13 to 22° in the three slightly different conformations found in its crystal structure. Nevertheless, since the closest approach distance between H(3) and H(9) is 2.3 Å, once again such a minimal steric interaction would not be expected to create a significant barrier to the rotation about the C(2)–C(8) bond. The 500 MHz ^1H NMR spectrum of **16** at 193 K exhibited no decoalescence or significant broadening of the phenyl peaks, suggesting a rotational barrier of less than 8 kcal mol⁻¹. This observation is in line with DFT calculations indicating a barrier of ca. 5 kcal

mol⁻¹ for a phenyl oscillation of the type illustrated in Scheme 5b.

As illustrated in Scheme 5, we note that the chromium complex **15** and the rhenium derivative **16** can both adopt mirror-symmetric (C_s) conformations. However, in the former case the indenyl moiety must lie orthogonal with respect to the phenyl ring plane (dihedral angle of 90°), whereas in **16** the molecular mirror plane bisects both ring systems when they are coplanar with a dihedral angle of 0° . We note parenthetically that detection of rotation of an η^5 -bonded organometallic fragment relative to an indenyl ring requires that the symmetry be lowered further, as for example in $(\eta^5\text{-1-methylindenyl})\text{Rh}(\text{C}_2\text{H}_4)_2$.¹⁷

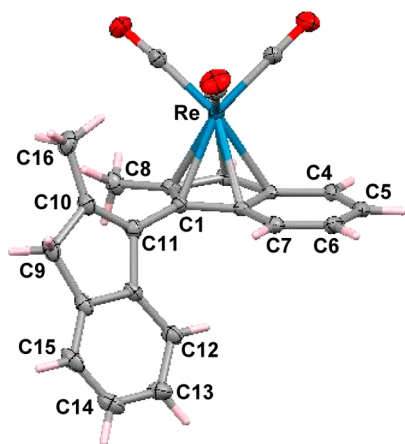
Hence, as given in Table 1, it is evident that the incorporation of an organometallic tripodal moiety does not per se impose a substantial energy barrier that markedly slows relative rotation of the adjacent aromatic systems. We now extend our focus to more complex systems bearing an organometallic tripod attached in an η^6 or η^5 fashion.

Recently, we described several interesting 2,2'-disubstituted 1,1'-biindenyls^{5c} that can exist in both meso and racemic forms. Rotation about the C(1)–C(1') linkage in these molecules is slow, owing to multiple side-to-side repulsions of the indenyl fragments and the substituents attached to the 2- and 2'-positions. Remarkably, when either *rac*- or *meso*-1,1'-di(2-methylindenyl) was heated with rhenium carbonyl in decalin at 160°C , an identical mixture of organorhenium products was formed. The major component of this mixture was found to be the monorhenium complex 1-(2-methylinden-3-yl)-2-methyl-1,2,3,3a,7a- $[\eta^5\text{-tricarbonylrhenium}]$ indenide (**17**), the molecular structure of which is shown in Figure 3. Formation of this rhenium tricarbonyl η^5 complex is accompanied by migration of the double bond in the five-membered ring of the second indenyl fragment, as seen previously in related systems.^{4,5a}

Table 1. Experimental and Calculated Rotational Barriers (kcal mol⁻¹) for Molecules Discussed in the Present Work

molecule	exptl (NMR) ^a	calcd (DFT)	comment
η^6 -[9-Cr@phenylanthracene] (19)	17.5	15.5	in 9-phenylanthracene the barrier is 21 kcal mol ⁻¹
η^6 -[9-(2-indenyl)anthracene]Cr (21)	14.5	13	in 9-(2-indenyl)anthracene the barrier is 12 kcal mol ⁻¹
η^5 -[9-(2-indenyl)anthracene]Cr (22)	13	11	slightly reduced barrier after $\eta^6 \rightarrow \eta^5$ migration
η^5 -[9-(2-indenyl)anthracene]Re (20)	11	9	isostructural with anionic chromium complex 22
η^6 -[9-(3-indenyl)anthracene]Cr (24)	>23	24	in 9-(3-indenyl)anthracene the barrier is 24 kcal mol ⁻¹
η^5 -[9-(3-indenyl)anthracene]Cr (25)	22	19	slightly reduced barrier after $\eta^6 \rightarrow \eta^5$ migration
η^5 -[9-(3-indenyl)anthracene]Re (23)	21.5	20.5 ^c	isostructural with the anionic chromium complex 25
η^6 -[9-Cr@phenyltriptycene] (27)	<i>b</i>	9	in 9-phenyltriptycene the barrier is <8 kcal mol ⁻¹
η^6 -[9-phenyl-Cr@triptycene] (28)	<8		
η^6 -[9-(2-indenyl)triptycene]Cr (1)	8		in 9-(2-indenyl)triptycene the barrier is <8 kcal mol ⁻¹
η^5 -[9-(2-indenyl)triptycene]Re (32)	19.5	20 ^c	isostructural with 2, the anion derived from 1; the $\eta^6 \rightarrow \eta^5$ migration yields an effective molecular brake!
η^6 -[9-(3-indenyl)triptycene]Cr (30)	<i>b</i>	17	in 9-(3-indenyl)triptycene the barrier is 12 kcal mol ⁻¹
η^5 -[9-(3-indenyl)triptycene]Re (33)	20	16.5 ^c	isostructural with the anion derivable from complex 30
η^6 -[9-(3-indenyl)Cr@triptycene] (31)	13	11.5	data from ref 5a

^aBarriers evaluated at T_c , the coalescence temperature. ^bHypothetical molecule. ^cCalculated for the analogous Mn(CO)₃ complex.

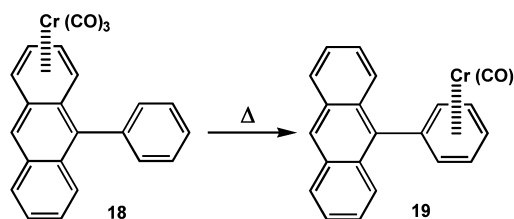
**Figure 3.** Molecular structure of the η^5 -Re(CO)₃ complex 17.

The ¹H–¹H 2D EXSY analysis of complex 17 at 323 K indicates a dynamic exchange process with a rotational barrier of ca. 20 kcal mol⁻¹. This value is in good agreement with a DFT computational study of 17, which revealed that a 360° rotation about the C(1)–C(11) single bond would evoke two substantial energy barriers, 20 and 24 kcal mol⁻¹, depending on whether the uncomplexed indenyl blade passes the C(8) methyl or the C(7) H in the complexed indenyl, thus making rotation in this system at room temperature very slow on the NMR time scale.

Internal Rotation in Metal Carbonyl Derivatives of Phenyl- and Indenylanthracenes. Our recent findings on

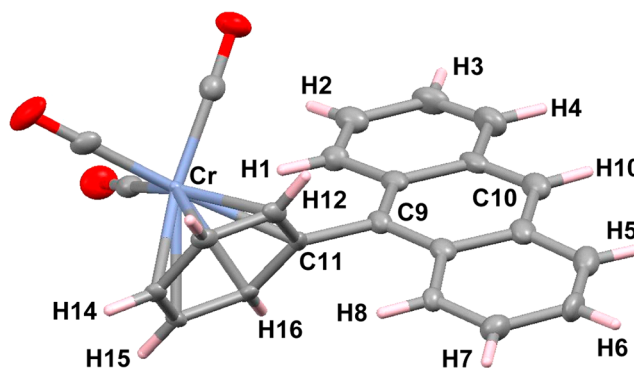
substituted anthracenes bearing a phenyl or 3-indenyl group at the 9-position suggest that strong double steric interactions between spatially adjoining hydrogens of the anthracene and phenyl or indenyl systems cause very significant rotational hindrance. As shown in Chart 1, rotational barriers increase rapidly in the order 3a < 5 < 3b, and we here analyze the manner in which attachment of an organometallic tripod to these aromatic skeletons can alter the internal rotation energy profile.

The formation of the tricarbonylchromium derivatives 18 and 19 from 9-phenylanthracene (5) has been previously reported to be a rather complex process.¹⁴ The initial purple Cr@anthracene η^6 complex 18 rearranges to furnish the yellow product 19 (Scheme 6). The yield of 19 is always poor, which

Scheme 6. Migration of a Cr(CO)₃ Moiety from a Peripheral Benzo Ring of Anthracene in 18 onto the 9-Phenyl Substituent in 19

may be attributable to the sterically shielded surroundings of the phenyl, whose aromatic system is tightly confined between the blades of the anthracene. In our hands, even after very careful adjustment of reaction conditions, the yield of 19 did not surpass 7%.

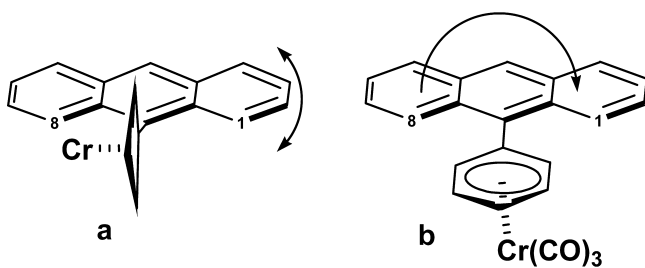
The structure of 19 has been determined by X-ray diffraction for the first time,¹⁸ and while a substantial degree of packing disorder prevents a precise determination of the molecular parameters, the data are sufficient to establish the molecular connectivity unequivocally (Figure 4). The phenyl and

**Figure 4.** Molecular structure of [η^6 -(9-anthracenyl)benzene]-tricarbonylchromium (19).

anthracenyl rings adopt a dihedral angle of approximately 60°, which may be compared to the structure of the related system 9-ferrocenylanthracene, in which the interplanar angle between the cyclopentadienyl and anthracene rings is 45°. We note that, were the solid state conformation of 19 to be retained in solution, the H(1) and H(8) positions of the anthracene should be rendered magnetically nonequivalent, and likewise for the H(12) and H(16) positions of the phenyl. The 500 MHz ¹H NMR spectrum of 19 at 25 °C revealed that the

resonances assignable to the H(1) and H(8) nuclei are separated by 1.42 ppm, a difference that can be attributed to the very significant diamagnetic anisotropy of the $\text{Cr}(\text{CO})_3$ group.¹⁰ However, H(12) and H(16), the ortho protons of the phenyl ring, remained isochronous. This nonequivalence of the anthracene blades, together with the apparent mirror symmetry of the phenyl ring, is consistent with a dynamic process whereby the phenyl- $\text{Cr}(\text{CO})_3$ unit is rapidly oscillating relative to the plane of the anthracene framework, as depicted in Scheme 7a. Since the 180° rotation of $\text{Cr}(\text{CO})_3@Ph$ ¹⁹ relative

Scheme 7. Proposed Dynamics of 19: (a) Oscillation of the Anthracene Close to the Perpendicular Orientation Leaves H(1) and H(8) Nonequivalent but Equilibrates the Edges of the Phenyl Ring and (b) Equilibration of the Terminal Benzo Rings of the Anthracene Requires a 180° Rotation of the Phenyl Ring To Generate Time-Averaged C_{2v} Symmetry



to the plane of the anthracene in 19 (Scheme 7b) would be expected to have to overcome a rather substantial energy barrier, this dynamic process was investigated by 2D ^1H - ^1H EXSY spectroscopy, which revealed an exchange process, $\text{H}(1) \leftrightarrow \text{H}(8)$, characterized by an activation energy of 17.5 ± 0.5 kcal mol⁻¹. It is noteworthy that this value is markedly lower than the corresponding barrier (21 kcal mol⁻¹) found in the parent hydrocarbon 9-phenylanthracene (5).^{5e}

It is apparent that rotation about the C(9)–C(11) single bond linking the phenyl and anthracene fragments in 19 is associated with strong steric interactions *in the plane* of the anthracene. Moreover, and somewhat contrary to expectations, the data available at present suggest that the presence of an η^6 -bonded tricarbonylchromium tripod in fact *reduces* the height of the barrier. This interesting finding will be considered further in the context of steric and electronic interactions in other metal tricarbonyl derivatives, as discussed below.

When 9-(2-indenyl)anthracene (3a) was heated with rhenium carbonyl in decalin at 160 °C, the η^5 derivative 20 was isolated in 22% yield. Analogously, the η^6 - $\text{Cr}(\text{CO})_3$ complex 21 was prepared in 95% yield by heating 3a with $\text{Cr}(\text{CO})_6$ in 1,4-dioxane at 120 °C. The structures of both complexes (Figure 5) display a slight twisting from planarity of the anthracene framework: by 11° in 20 and by 3° in 21. Such minor perturbations may arise through π -stacking or other crystal-packing effects. The interplanar indenyl–anthracene angles are 52° (20) and 62° (21), thus rendering the peripheral blades of the anthracene nonequivalent in the solid state.

As shown in Figure 6a, at 193 K the 500 MHz ^1H NMR spectrum of the rhenium complex 20 in CD_2Cl_2 exhibited

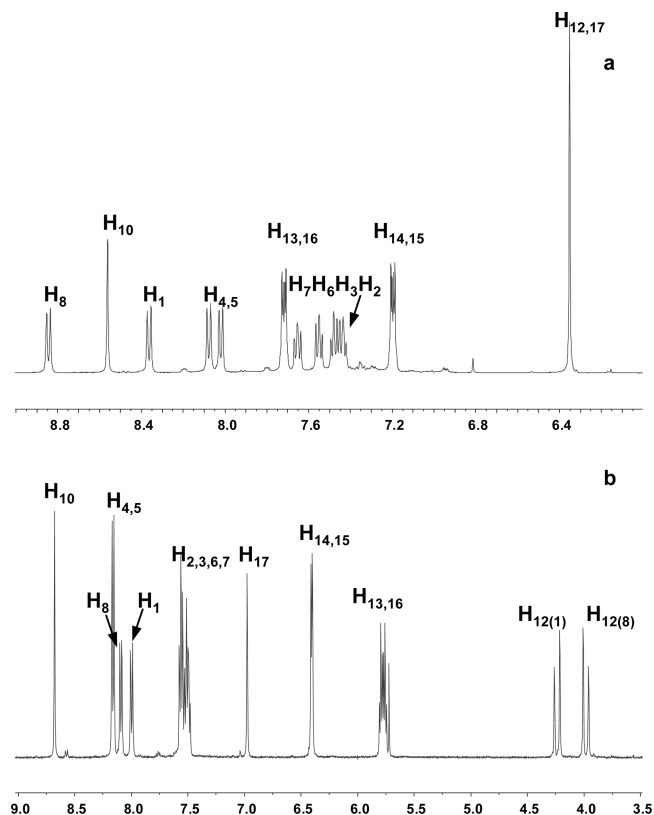


Figure 6. Sections of the 500 MHz ^1H NMR spectra of (a) the η^5 -Re complex 20 at 193 K in CD_2Cl_2 and (b) the η^6 -Cr complex 21 at 243 K in acetone (atom numbering as in Figure 5).

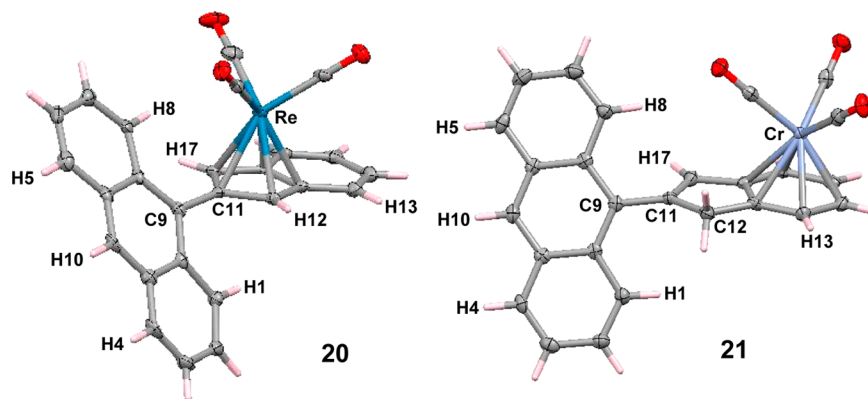


Figure 5. Molecular structures of $[\eta^5\text{-}2\text{-(9-anthracenyl)indenyl}]$ tricarbonylrhenium (20) and $[\eta^6\text{-}2\text{-(9-anthracenyl)indene}]$ tricarbonylchromium (21).

doublets for the anthracene protons H(1) and H(8) at 8.35 and 8.85 ppm, respectively. This very marked chemical shift difference can be attributed to the large diamagnetic anisotropy of the adjacent $\text{Re}(\text{CO})_3$ tripod. Coalescence of these peaks at 243 K indicated a barrier of $11.1 \pm 0.5 \text{ kcal mol}^{-1}$ for anthracene rotation. However, no broadening of the indenyl five-membered-ring signals at H(12)/H(17) was observed even at 193 K, indicating that oscillation of the indenyl- $\text{Re}(\text{CO})_3$ unit about the mirror plane containing the anthracene framework remains fast on the NMR time scale, analogously to the behavior of 9-phenylanthracene- $\text{Cr}(\text{CO})_3$ (**19**), as depicted in Scheme 7.

In the chromium complex **21** the degeneracy of the anthracenyl H(1) and H(8) protons is again split at low temperature; however, the shift separation is now only 0.07 ppm, reflecting the greater distance from the $\text{M}(\text{CO})_3$ moiety. Peak coalescence data (see the Supporting Information) yield a barrier of $14.7 \pm 0.5 \text{ kcal mol}^{-1}$ for equilibration of the outer rings of the anthracene. The placement of the π -bonded organometallic fragment on one face of the indene “paints the faces different colors”²⁰ and so renders diastereotopic the methylene protons at C(12). It is well established that the diamagnetic anisotropy of the $\text{Cr}(\text{CO})_3$ tripod preferentially deshields the endo proton relative to its exo counterpart,²¹ thus allowing their ready attribution as H(12)_{exo} and H(12)_{endo} at 3.98 and 4.26 ppm, respectively. Subsequent NOE measurements indicated pairwise interactions between the peaks at 4.26 and 8.01 ppm and those at 3.98 and 8.08 ppm, thus allowing the attribution of H(8) as being more shielded than H(1). It appears likely that the favored conformation in solution parallels that found in the solid state, whereby the dihedral angle between the indenyl and anthracenyl ring planes is 62° .

It is particularly noteworthy that the barrier for anthracene rotation in the rhenium η^5 complex **20** is approximately $3.5 \text{ kcal mol}^{-1}$ lower than that found in the closely related chromium η^6 complex **21**, despite the fact that the metal tripod is considerably closer to the anthracene system in the former case. Interestingly, this finding is in good agreement with DFT calculations showing that the rotational barrier is $4.4 \text{ kcal mol}^{-1}$ lower for the η^5 -Re system **20** than for the η^6 -Cr complex **21**. However, one should recall that the NMR experiment merely yields a value for the energy separation between the ground state and the transition state for the dynamic process. One cannot assume that moving the metal tripod closer to the rotating group actually lowers the energy of the transition state; it is perhaps more likely that steric interactions raise the energy of the ground state.

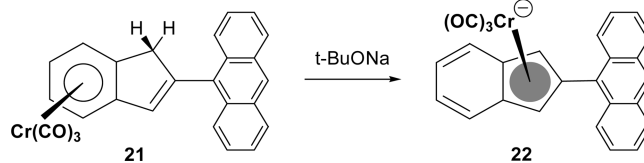
These findings on the organometallic systems **19–21**, whereby a five- or six-membered ring bearing a metal tricarbonyl tripod is attached to the 9-position of anthracene, may be compared to the previously reported molecules **3a,b**, **5**, and **7** (Chart 1), as these relationships have important implications for the understanding of the function of haptotropic molecular brakes such as **1**. The new data reveal that the introduction of a metal carbonyl moiety does not in itself lead to an increase of the rotational barrier; indeed, in (9-phenylanthracene) $\text{Cr}(\text{CO})_3$ (**19**, with $\text{Cr}@\text{Ph}$), the value of ca. $17.5 \text{ kcal mol}^{-1}$ is noticeably less than that reported (21 kcal mol^{-1}) for the uncomplexed hydrocarbon **3**.^{5c} While this result may be related to a somewhat raised value for complex **19** in its minimum energy conformation, one must also consider possible stabilization of its highly distorted transition state by the metal carbonyl. We have shown previously in 9-phenyl-

anthracene (**3**)^{5c} and also in 9-ferrocenylanthracene (**7**)⁶ that as the dihedral angle between the rotating fragments approaches 0 , the molecular geometry of the hydrocarbon framework is forced to deviate quite significantly from coplanarity.

Furthermore, and in line with our recent findings,^{5,6} it has been shown that the rotational barriers themselves appear to arise from the interactions of the peri-oriented H(1) and H(8) atoms of the anthracene with the five- or six-membered ring rather than with the metal tricarbonyl unit attached to the scaffold in a perpendicular direction. This phenomenon may also provide a simple rationale for a longstanding observation of the relative barriers to rotation in ferrocenylpentaphenylbenzene²² and (hexaphenylbenzene)tricarbonylchromium, where the $\text{Cr}(\text{CO})_3$ is π -bonded to one of the peripheral phenyls.²³ In the latter case, the barrier to rotation of the $(\text{C}_6\text{H}_5)_3\text{Cr}(\text{CO})_3$ substituent is 12 kcal mol^{-1} ,²³ whereas in the former system the barrier to rotation of the ferrocenyl group relative to the central ring was too low to be determined by variable-temperature NMR measurements.²² Discussion at that time focused on the cone angles swept out by the phenyl- $\text{Cr}(\text{CO})_3$ and ferrocenyl groups, but a more prosaic explanation merely involves the fact that the five-membered ring poses less steric interaction than the six-membered ring as it approaches coplanarity with the central ring; in these cases, the organometallic fragment— $\text{Fe}(\text{C}_5\text{H}_5)$ or $\text{Cr}(\text{CO})_3$ —merely serves as a label to lower the symmetry and so allows the dynamic process to be monitored.

(η^6 -2-(9-Anthracenyl)indenyl)tricarbonylchromium(0) (21**) as a Molecular Shuttle.** The known ability of a tricarbonylchromium unit to undergo an η^6 to η^5 haptotropic shift across an indenyl framework prompted us to investigate the possibility of molecular shuttling in **21**. In principle, such a process (Scheme 8) would furnish **22**, the anionic $\text{Cr}(\text{CO})_3$ analogue of the η^5 - $\text{Re}(\text{CO})_5$ complex **20**.

Scheme 8. Haptotropic Shift from the η^6 -Indene Complex **21** to the η^5 -Indenyl Anion **22**



Indeed, when sodium *tert*-butoxide was added to a solution of **21** in DMSO, the ^1H NMR spectrum (Figure 7) recorded after 12 h clearly revealed the formation of the anticipated η^5 - $\text{Cr}(\text{CO})_3$ anionic complex **22**. Since the doublet resonance at 9 ppm attributable to H(1) and H(8) is not significantly

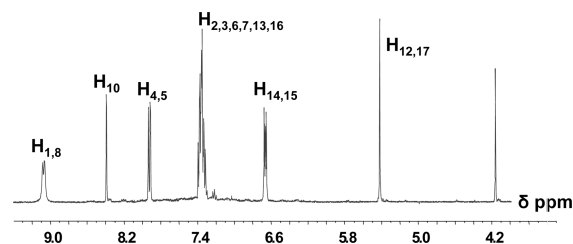


Figure 7. 500 MHz ^1H NMR spectrum of $\text{Na}^+[\{\eta^5\text{-2-(9-anthracenyl)indenyl}\}\text{Cr}(\text{CO})_3]^-$ (**22**) (atom numbering as for molecule **20** in Figure 5).

broadened at 303 K, this may imply a *lower* rotational barrier in the η^5 complex **22** than in the parent η^6 complex **21**; however, in this case the barrier cannot be precisely determined, as the DMSO solvent freezes at 290 K. Strikingly, the behavior of the potential anthracene-based molecular brake, **21/22**, contrasts with that of the triptycene-based molecular brake, **1/2**, for which the η^5 complex has an enormously enhanced rotational barrier. Hence, even though both systems incorporate the same molecular actuator, i.e. a sliding chromium tricarbonyl moiety attached to the 2-indenyl fragment, this demonstrates the very different behavior of the two-bladed (anthracenyl) and three-bladed (triptycyl) molecular rotors.

Chromium and Rhenium Tricarbonyl Derivatives of 3-Indenylanthracenes. Analogously to the reactions of 2-indenylanthracene (**3a**) with metal carbonyls, isomeric 3-indenylanthracene (**3b**) was also converted into its rhenium η^5 - $\text{Re}(\text{CO})_3$ complex **23** (12% yield) and the η^6 - $\text{Cr}(\text{CO})_3$ derivative **24** (57% yield). Interestingly, although the solid-state structures of **23** and **24** are superficially very similar (Figure 8), there are some significant differences. If one were to

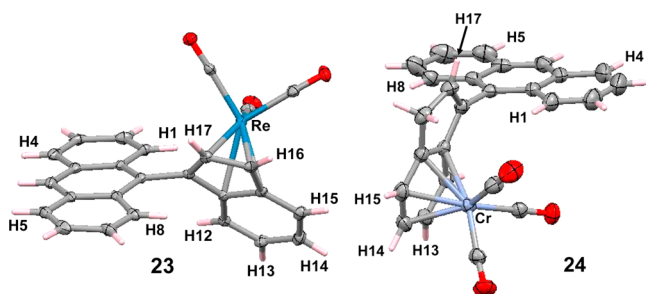


Figure 8. Molecular structures of $[\eta^5\text{-}3\text{-(9-anthracenyl)indenyl}]$ -tricarbonylrhenium (**23**) and $[\eta^6\text{-}3\text{-(9-anthracenyl)indene}]$ -tricarbonylchromium (**24**).

imagine the anthracenyl unit initially positioned orthogonally to the plane of the indenyl/indene framework, then in the rhenium complex **23** the proximal face of the indenyl- $\text{Re}(\text{CO})_3$ unit has rotated 56.5° toward the anthracene, whereas in the chromium system the indenyl fragment has rotated 75.5° away from the plane of the anthracene.

The 500 MHz ^1H NMR spectra of **23** and **24** are shown in Figure 9. In the rhenium complex **23**, the anthracene peri protons, H(1) and H(8), are widely separated (9.42 and 7.25 ppm, respectively). The lower field resonance, H(1), is clearly in the deshielding region of the $\text{Re}(\text{CO})_3$ tripod and shows an NOE interaction with H(12) in the indenyl six-membered ring. Concomitantly, H(8) is proximate to H(17), the five-membered-ring proton adjacent to the C(9)–C(11) bond linking the indenyl and anthracenyl units. Since the X-ray crystal structure reveals the distance between these NOE-connected pairs of protons to be ca. 2.47 Å, it is apparent that the conformations found in the solid state are also favored in solution.

We have previously reported that rotation of the 3-indenyl moiety in the parent hydrocarbon **3b** has a barrier of 25 kcal mol $^{-1}$, and so NMR peak coalescence is unattainable at accessible temperatures.^{5d} Assuming comparable barriers for **23** or **24**, their dynamics were probed by using 2D EXSY at 323 K. Gratifyingly, rotation of the anthracene moiety in the η^5 - $\text{Re}(\text{CO})_3$ complex **23** was detectable at this temperature, and off-diagonal exchange peaks for H(1) \leftrightarrow H(8) and H(2) \leftrightarrow H(7) were clearly evident. Quantitative analysis of the data yielded a rotational barrier of 21.5 ± 0.5 kcal mol $^{-1}$, noticeably lower than in 3-indenylanthracene itself. In contrast, a 2D-EXSY study of the η^6 - $\text{Cr}(\text{CO})_3$ derivative **24** failed to identify any exchange process even at 323 K, thus indicating a rotational barrier in excess of 23 kcal mol $^{-1}$.

Continuing our study of haptotropic shuttling of metal tricarbonyl moieties from a six- to a five-membered ring, as depicted in Scheme 9, when sodium *tert*-butoxide was added to a DMSO solution of **24**, the η^6 - $\text{Cr}(\text{CO})_3$ derivative of 3-

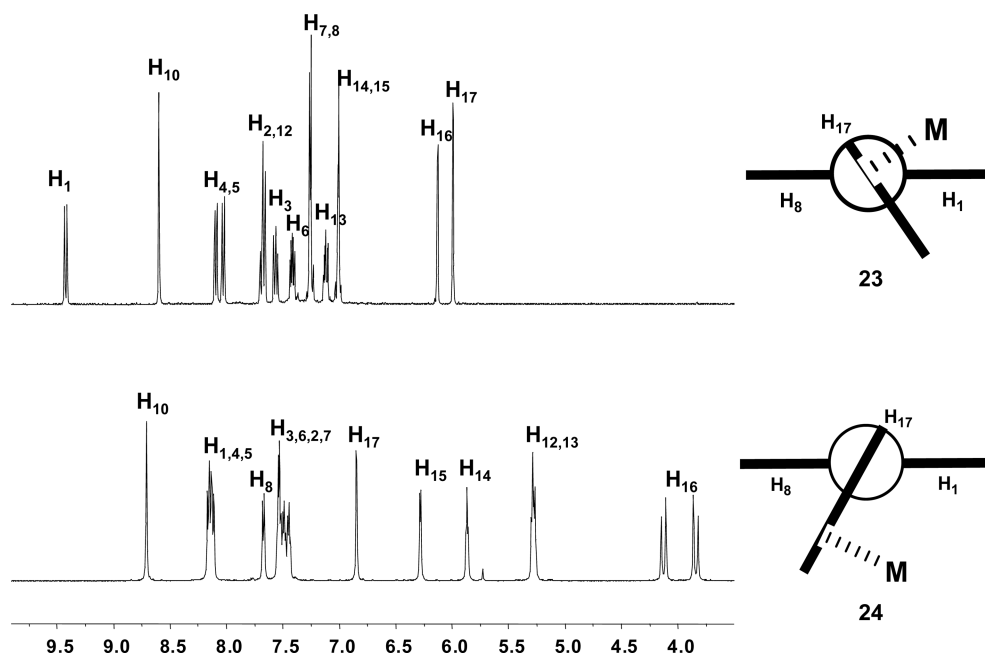
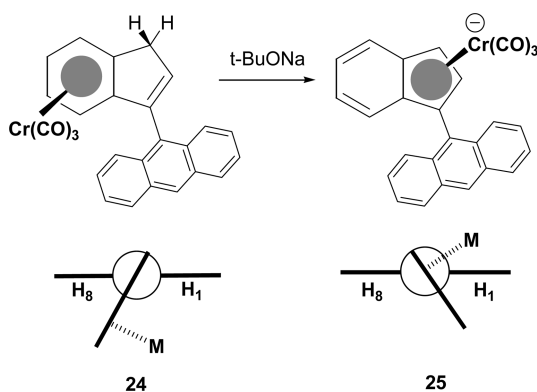


Figure 9. 500 MHz ^1H NMR spectra and proposed conformations in solution of the Re and Cr complexes **23** and **24**, as determined by 2D ^1H - ^1H NOESY measurements at 303 K.

Scheme 9. Haptotropic Shift of the $\text{Cr}(\text{CO})_3$ Unit in **24** To Form **25** Also Accompanied by a Conformational Change



indenylanthracene, the ^{13}C NMR spectra recorded after 12 h (Figure 10) clearly showed the formation of a new anionic

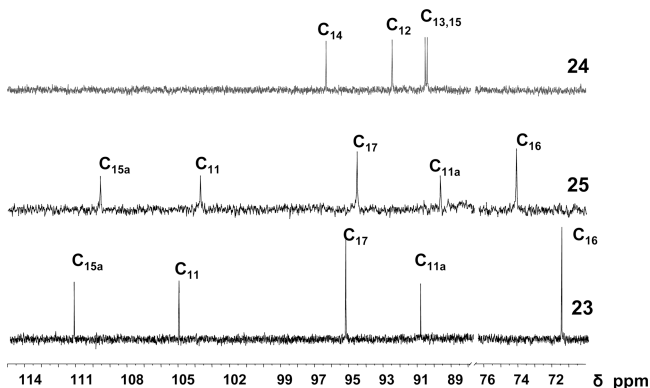


Figure 10. Spectroscopic ^{13}C NMR (DMSO, 303 K) observation of a rearrangement of the chromium complex **24** into the anionic system **25**, isostructural with the rhenium complex **23**.

complex, **25**, isostructural with the rhenium complex **23**. Moreover, the ^1H 2D NOESY study revealed that complex **25** adopted a conformation very similar to that of the η^5 -rhenium complex **23** (Figure 8), in which H(17) at 5.10 ppm is proximal to H(8) at 7.46 ppm; likewise, H(12) and H(1) at 6.68 and 10.60 ppm, respectively, are close neighbors in space. 2D EXSY data on **25** revealed exchange peaks for H(1) \leftrightarrow H(8) and H(2) \leftrightarrow H(7); the rotational barrier was found to be 22 ± 0.5 kcal mol $^{-1}$, slightly lower than in the precursor η^6 complex **24** and close to the value (21.5 kcal mol $^{-1}$) previously seen in the η^5 -Re analogue **23**.

Our results on the systems **23**–**25** can be compared to those for the parent hydrocarbon, 3-indenylanthracene (**3b**), in which the rotation of the indenyl moiety, although not directly measurable, is believed to be slow with a 25 kcal/mol barrier.^{5d} As in the case of 2-indenyl derivatives, our findings appear to suggest that the introduction of a metal carbonyl moiety attached at the five-membered ring of **3b** significantly decreases the rotational barrier. It is reasonable to assume that, similarly to the 2-indenylanthracene metal complexes **20** and **22**, the rotational barriers in **23** and **24** also arise from the interactions of the peri-oriented H(1) and H(8) of the anthracene with the five- and six-membered rings rather than the metal tricarbonyl unit attached to the scaffold in a perpendicular direction. As noted above, the apparent decrease of the rotational barrier in

the η^5 complexes relative to that of their noncomplexed precursors may be a consequence of raising the energy of the ground state and/or metal carbonyl stabilization of the highly distorted transition state. The DFT calculated rotational barriers in these systems (Table 1) indicate that the barrier in the η^6 complex **24** is very similar to that of the parent hydrocarbon **3b**, whereas the calculated barrier in the η^5 analogue **23** is lower by ca. 3.5 kcal mol $^{-1}$.

Internal Rotation in Metal Carbonyl Derivatives of Aryl-Substituted Three-Blade Systems. It has been shown in the previous section that haptotropic translational movement of a metal tricarbonyl unit from the six- to the five-membered ring of an indenyl fragment attached to anthracene at the 9-position does not increase the barrier to the rotation; indeed, there are indications that this barrier is somewhat reduced. In contrast, in the analogous indenyltritycene complexes, the same metal tricarbonyl moiety effectively blocks rotation of the paddlewheel, as the barrier in the η^5 complex is at least 12 kcal mol $^{-1}$ higher than that in the η^6 counterpart.

As shown in Chart 1, the barrier to rotation about the 3-fold axis in 9-substituted triptycenes increases markedly from the 2-indenyl derivative **4a** to the isomeric angular system **4b**, in which the six-membered ring of the indene is directly adjacent to the blades of the triptycene. However, this increase in the height of the barrier is even greater when the 9-substituent possesses an orthogonally attached fragment, such as $\text{Re}(\text{CO})_3$ in **2** or $\text{Fe}(\text{C}_5\text{H}_5)$ in **8**. To probe more deeply into this phenomenon, we have synthesized and characterized several systems in which an aryl- $\text{M}(\text{CO})_3$ moiety is connected to a nominally C_3 -symmetrical rigid hydrocarbon skeleton, namely triptycene or [2.2.2]bicyclooctane. In addition, their dynamic behavior was investigated by experiment, by NMR spectroscopy, and also by means of DFT calculations.

When 1,4-diphenylbicyclo[2.2.2]octane (1,4-diphenyl-BCO) and $\text{Cr}(\text{CO})_6$ were heated in dioxane at 120 °C for 24 h, the monochromium derivative **26** was obtained in 45% yield. Its molecular structure appears in Figure 11, from which it is

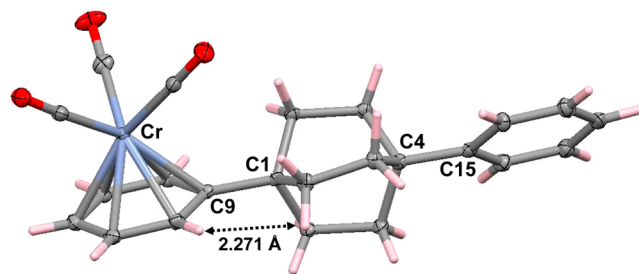


Figure 11. Molecular structure of (η^6 -1,4-diphenylbicyclo[2.2.2]octane) $\text{Cr}(\text{CO})_3$ (**26**).

apparent that rotation of the C_6H_5 - $\text{Cr}(\text{CO})_3$ unit would not evoke contacts shorter than 2.2 Å between the hydrogen atoms of the BCO core and the coordinated phenyl ring. Additionally, the hydrocarbon backbone of the molecule, i.e. C(9)–C(1)–C(4)–C(15), deviates only 2° from linearity. Accordingly, one would anticipate a barrier to rotation about the C(1)–C(9) single bond of less than 8 kcal mol $^{-1}$; a DFT calculation yielded a value of ca. 6 kcal mol $^{-1}$, and the 500 MHz ^1H NMR spectrum at 193 K did not exhibit peak decoalescence. One may conclude that incorporation of a $\text{Cr}(\text{CO})_3$ tripod to an aromatic group directly linked to the C_3 -symmetrical BCO

scaffold does not bring about a substantial increase in the aryl rotational barrier.

With the goal of extending this topic from a bicyclo[2.2.2]-octane to the bulkier triptycene system, an attempt was made to prepare $(\eta^6\text{-9-phenyltriptycene})\text{Cr}(\text{CO})_3$ such that the metal was π -bonded to the phenyl substituent, as in **27**. However, when the reaction was performed, it yielded only the isomeric complex **28**, whereby the $\text{Cr}(\text{CO})_3$ fragment was attached to a blade of the triptycene (Figure 12). In unsubstituted

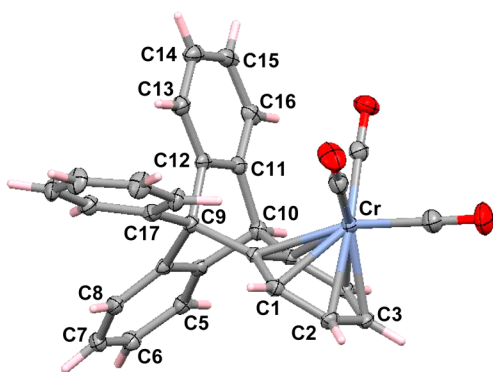


Figure 12. Molecular structure of the chromium complex **28**.

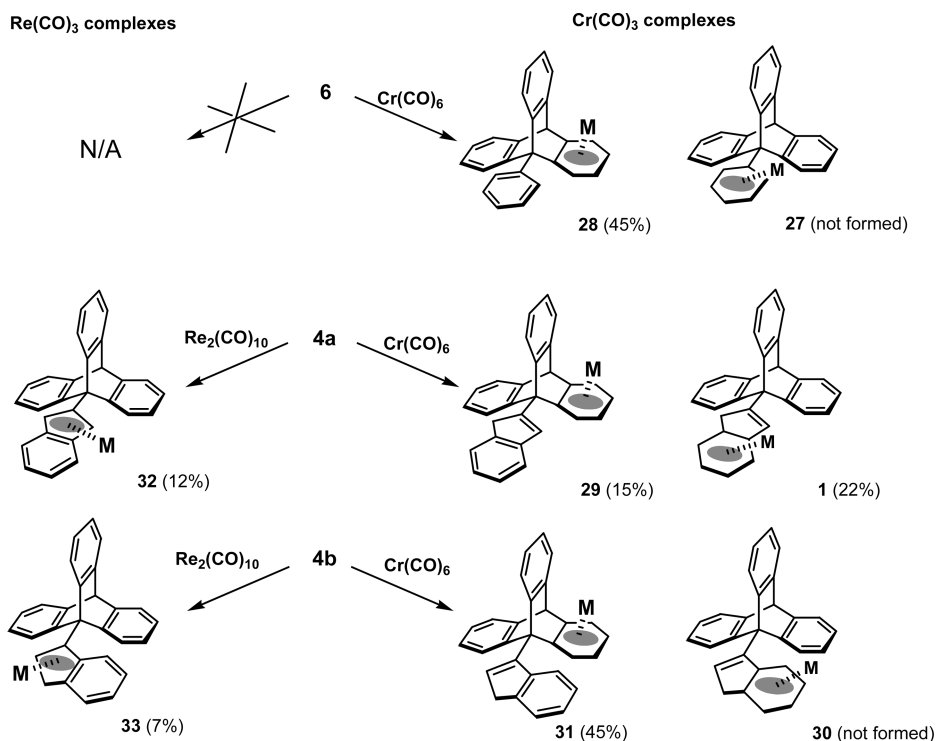
triptycenes bearing tricarbonylchromium fragments, breaking the 3-fold symmetry did not greatly change the interblade angles, which ranged only from 117.7 to 121.9°. ^{13a,24} However, as previously noted in $\eta^6\text{-[9-(3-indenyl)Cr@triptycene]}$, ^{5a} the 3-fold symmetry in **28** is indeed seriously perturbed; the valley containing the organometallic unit widens to 134.5°, while the other two diminish accordingly, with dihedral angles of 102.1 and 123.4°.

This observation contrasts with the situation previously reported in the reaction of $\text{Cr}(\text{CO})_6$ with 9-(2-indenyl)-triptycene (**4a**), for which two complexes have been isolated. As shown in Scheme 10, in **29** the $\text{Cr}(\text{CO})_3$ is bonded to a triptycene blade; in **1**, the tripod is η^6 linked to the six-membered ring of the indenyl substituent. ⁴ However, the reactivity of 9-(3-indenyl)triptycene (**4b**) parallels that of 9-phenyltriptycene (**6**), such that it does not form the Cr@ indene complex **30** but instead yields the blade-bonded isomer **31**. ^{5a} Apparently, spatial proximity of the target benzene ring to the triptycene paddlewheel unit sterically precludes the formation of chromium tricarbonyl complexes **27** and **30**. Unfortunately, the alternative route to these hypothetical complexes via benzyne addition to their corresponding precursor anthracenes was not successful, and mixtures of unidentified products were obtained.

Upon examination of the molecular structure of **28**, the triptycene blade bonded $\text{Cr}(\text{CO})_3$ complex shown in Figure 12, one would not anticipate a substantial barrier toward the rotation of the 9-phenyl substituent. The position and orientation of the phenyl are almost identical with those recently found in the parent structure **6**; ^{5d} for example, the C(10)–C(9)–C(17) angle is 174° in both cases. Accordingly, NMR measurements revealed that, while all three blades of the triptycene are, of course, nonequivalent, the phenyl substituent displays dynamic C_{2v} symmetry, showing that it is freely rotating about the C(9)–C(17) axis on the NMR time scale. Similar structural and dynamic relationships have previously been reported for the blade-bonded $\text{Cr}(\text{CO})_3$ complex **31** and its parent compound 9-(3-indenyl)triptycene (**4b**), which both displayed rotational barriers of $\sim 12.5 \text{ kcal mol}^{-1}$. ^{5a}

Having established the experimental inaccessibility of the chromium derivatives **27** and **30**, whereby the metal was positioned on the 9-phenyl or 9-(3-indenyl) substituent of the

Scheme 10. Possible Metal Carbonyl Derivatives of the Triptycenes **4a,b** and **6**



tritycenes **4b** and **6**, respectively, we turned instead to η^5 complexes such that a tricarbonylrhenium tripod is located on the five-membered ring of the indenyl (see Scheme 1). Indeed, the $[\eta^5\text{-2-indenyltritycene}]M(\text{CO})_3$ complex **32** ($M = \text{rhenium, manganese}$) has previously served as a convenient isolobal, structural, and dynamic model of the anionic chromium species **2** (Scheme 1).⁴

Prolonged heating of 9-(3-indenyl)tritycene (**4b**) with $\text{Re}_2(\text{CO})_{10}$ in decalin at 180 °C furnished the complex **33** in 7% yield; the structure, shown in Figure 13, clearly illustrates

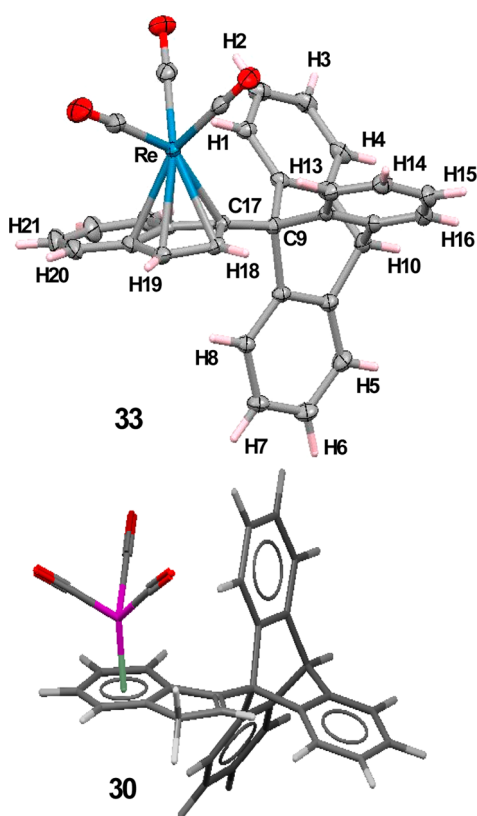


Figure 13. Molecular structure of the η^5 -rhenium complex **33** and DFT-optimized structure of the experimentally unavailable η^6 -chromium complex **30**. These views illustrate the spatial relationships between the two molecules and are also consistent with the EXSY data shown in Figure 14.

the nonequivalence of the three aromatic blades of the triptycene. Unlike in the parent system **4b**, where the plane of the indenyl is almost coplanar with one of the triptycene blades, instead in **33** the indenyl ring is now perpendicular to one of the blades, thus aligning the $\text{Re}(\text{CO})_3$ tripod with a valley between the other two blades. In the solid state, two of the three carbonyl ligands are pointing toward their adjacent blades, thus engendering steric strain, as evidenced by the deviation of the indenyl plane from the nominal 3-fold axis of the triptycene by 21° (this deviation is only 9° in **4b**). Since the observed molecular structure of **33** is in good agreement with that predicted by DFT, the structure of the hypothetical $\text{Cr}(\text{CO})_3$ complex **30** was also optimized by calculation and is shown in Figure 13 (lower structure). In this case, although the orientation of the indene relative to the triptycene blades is similar to that seen in complex **33**, the deviation of the indene plane from the triptycene axis is negligible, indicating very little

steric interaction between the triptycene moiety and the metal tricarbonyl tripod.

The dynamic behavior of the triptycene paddlewheel in the $\eta^5\text{-Re}(\text{CO})_3$ complex **33** was further probed by ^1H NMR spectroscopy at 303 K, which revealed the expected nonequivalence of the three triptycene blades. As a result of the diamagnetic anisotropy of the cyclopentadienyl- $\text{Re}(\text{CO})_3$ moiety, the chemical shifts of the three ortho hydrogens H(1), H(8), and H(13) are widely separated: H(8) located under the five-membered ring is at 5.85 ppm, while the two remaining hydrogens resonate at 8.15 and 7.77 ppm.

As these three proton environments do not exhibit coalescence even at 363 K, the 2D-EXSY spectrum of **33** was recorded at 323 K with a 1 s mixing time. As shown in Figure 14, the existence of the relevant off-diagonal peaks unequiv-

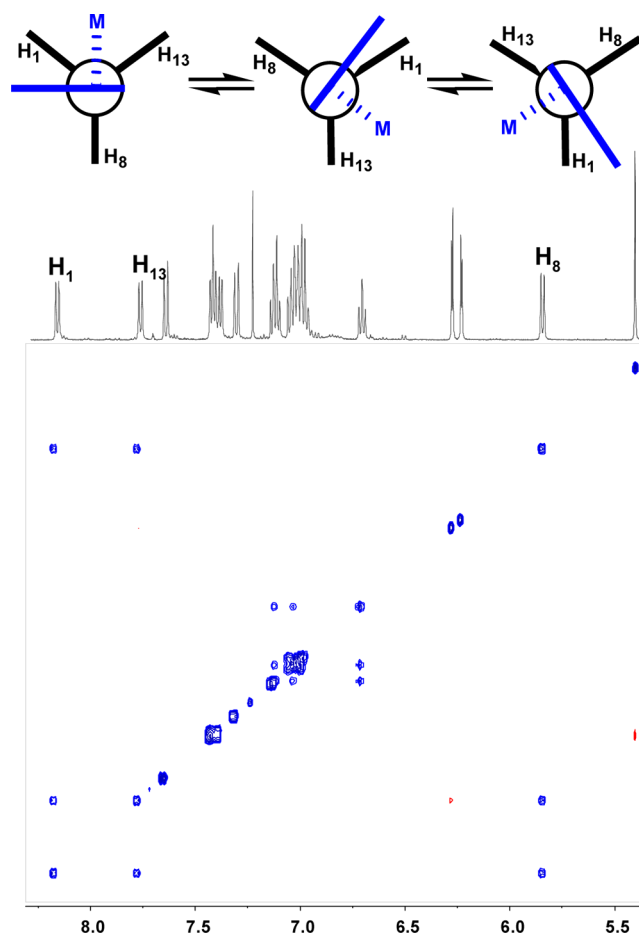
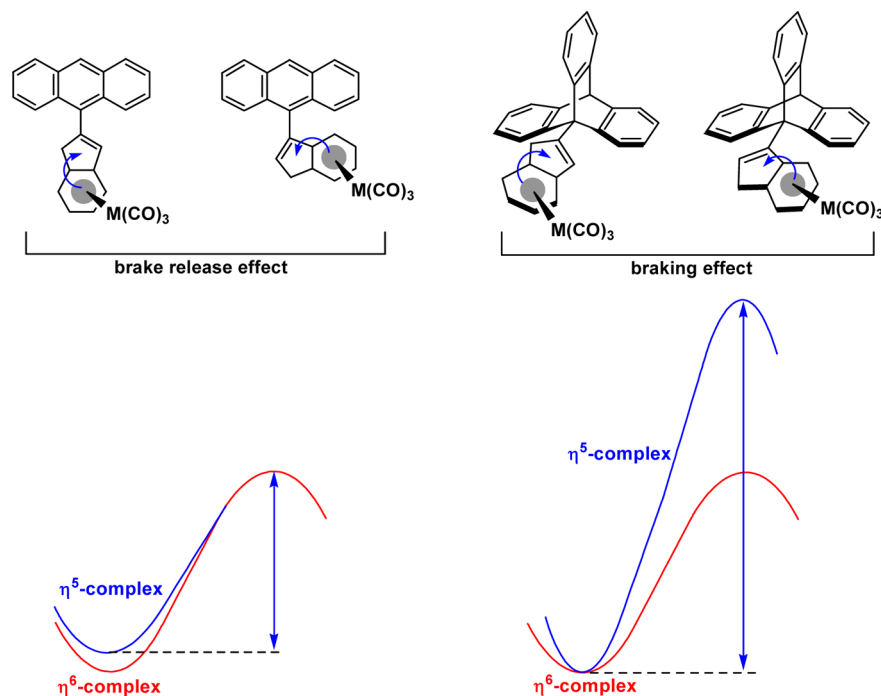


Figure 14. 2D ^1H - ^1H EXSY spectrum of $[\eta^5\text{-3-(9-tritycyl)indenyl}]\text{-Re}(\text{CO})_3$ (**33**) (323 K, $T_m = 1000$ ms, CDCl_3) exhibiting cross-peaks showing exchange between all three nonequivalent aromatic blades of the triptycene paddlewheel.

ocally demonstrates exchange between these sites via 120° rotations. Quantification of 2D-EXSY data over the temperature range 303–323 K yielded a rotational barrier of 20 ± 0.5 kcal mol⁻¹.

Comparing the results of the DFT calculated rotational barriers for the anthracenes and triptycenes and their metal tricarbonyl complexes, it is evident that the values for the hydrocarbons can be predicted with a substantial degree of accuracy. However, comparison of the DFT B3LYP calculated values and experimental free energies for the metal tricarbonyl

Scheme 11. On Account of the Higher Ground State Energy of the η^5 Complexes, an $\eta^6 \rightarrow \eta^5$ Haptotropic Migration of the Metal Tricarbonyl Unit in 9-Anthracene Derivatives Resulted in a Slight Lowering of the Observed Paddlewheel Rotational Barrier; Conversely, $\eta^6 \rightarrow \eta^5$ Haptotropic Shifts in the Analogous 9-Triptycene Derivatives Led to a Marked Increase of This Barrier



derivatives **19–34** (Table 1) suggests that in most cases the calculated energy barriers are lower than the experimental values. This difference ranges from 1.5 to 3.0 kcal mol⁻¹ for the anthracene derivatives **19–25** but more significantly up to 3.5 kcal mol⁻¹ for the triptycene derivative **31**, possibly owing to considerable distortion of the metal carbonyl fragment in the transition state. Indeed, in those cases with large barriers the molecules may become significantly more crowded at the rotational transition states, thus decreasing the entropy, making $-T\Delta S$ positive, and increasing the free energies of activation.

Nevertheless, comparison of the rotational barriers within either the experimental or the calculated data set shows that attachment of a metal tricarbonyl fragment to 9-arylanthracene and 9-aryltriptycene systems does not significantly alter their rotational freedom unless the metal carbonyl tripod is connected in such a fashion that it is adjacent to the 9-position of the anthracene or triptycene. One may summarize as follows.

- (1) Rotational barriers in the η^5 derivatives of 9-indenylanthracenes **20**, **22**, **23**, and **25** are somewhat *lower* than in their parent hydrocarbons or the corresponding η^6 -complexes **21** and **24**, possibly rationalizable in terms of a higher ground state energy rather than a reduced energy transition state. Consequently, an $\eta^6 \rightarrow \eta^5$ haptotropic migration of the metal tricarbonyl fragment *closer* to the rotatable single bond leads to a relatively somewhat diminished braking effect or “brake release” effect, as shown in Scheme 11.
- (2) Rotational barriers in the η^5 complexes of the 9-indenyltriptycenes **29** and **31** and the hypothetical **34** are considerably *higher* than in their precursor η^6 complexes, thus leading to a pronounced braking effect due to simultaneous multiple steric interactions of the metal carbonyl tripod and the five-membered ring of the

indenyl moiety with the adjacent H(1), H(8), and H(13) positions of the triptycene. Experimentally, as shown in Scheme 1, the rotation of the triptycene paddlewheel is slowed by a factor of ca. 10⁸.

To conclude, polycyclic hydrocarbons in which two aromatic or rigid aliphatic moieties are connected by a single C–C bond provide interesting molecular systems for the study of rotational barriers. A series of η^6 - and η^5 -M(CO)₃ derivatives of such hydrocarbons have been synthesized and characterized by X-ray crystallography and their dynamic behavior has been studied both by experiment and by means of DFT calculations. Several of these systems are potential candidates as mechanically controlled intramolecular rotation systems (molecular brakes). Somewhat unexpectedly, for indenylanthracenes slightly reduced rotational barriers were found for the η^5 complexes relative to their η^6 precursors or the respective uncomplexed hydrocarbons. The rotational barriers in such systems are controlled largely by strong double steric clashes between the quasi-planar indenyl moiety and the peri positions of the anthracene. In contrast, in the 2- and 3-indenyltriptycenes, significantly higher barriers (ca. 20 kcal mol⁻¹) have been observed and/or calculated for the η^5 -M(CO)₃ complexes than for the corresponding η^6 -M(CO)₃ complexes (8–10 kcal mol⁻¹). This very pronounced molecular braking effect attributable to multiple steric interactions between the triptycene paddlewheel and the indenyl-metal tricarbonyl moiety has so far been established only for triptycene derivatives, but work is underway to extend this fascinating effect to other three-bladed molecular paddlewheels.

■ EXPERIMENTAL SECTION

General Methods. All reactions were carried out under a nitrogen atmosphere unless otherwise stated. Column chromatography

separations were carried out on a Buchi Sepacor machine with UV absorbance detector using silica gel (particle size 40–63 mm). NMR spectra were acquired on Varian VnmrS 400, 500, and 600 MHz spectrometers at 30 °C unless otherwise stated; dynamic variable-temperature studies within the temperature range 193–363 K were carried out on a Varian Inova 500 MHz instrument. Assignments were based on standard ^1H – ^1H and ^1H – ^{13}C two-dimensional techniques and NOE measurements. Melting points were determined on a Gallenkamp instrument in air and are uncorrected. Elemental analyses were carried out by the Microanalytical Laboratory at University College Dublin.

Compounds **3a,b**, **4b**, **5**, **6**, 2-phenylindene (**35**), and 2,2'-dimethyl-1,1'-biindenyl (**36**) were prepared as described elsewhere.^{5,6}

Synthesis of $[\eta^6\text{-2-Methylindene}]_2\text{tricarboxylchromium}$ (13**).** 2-Methylindene (65 mg, 0.5 mmol) was heated with $\text{Cr}(\text{CO})_6$ (220 mg, 1 mmol) in dioxane (2 mL) at 125 °C in a sealed tube for 1 day, and the products were separated chromatographically (eluent ethyl acetate/cyclohexane) to give **13** (70 mg, 0.26 mmol, 52%) as a yellow solid. ^1H NMR (400 MHz, $\text{DMSO}-d_6$, 30 °C, numbering in accord with Figure 1): δ 6.27 (1H, s, H_3), 6.19 (1H, d, $J = 6$ Hz, H_7), 6.02 (1H, d, $J = 6$ Hz, H_4), 5.55 (1H, t, $J = 6$ Hz, H_5), 5.53 (1H, d, $J = 6$ Hz, H_6), 3.57 and 3.28 (2H, each d, $J = 23$ Hz, H_{11} , $\text{H}_{1'}$), 2.06 (3H, s, H_8). ^{13}C NMR (100 MHz): δ 235.6 (Cr-CO's), 151.6 (C_2), 124.1 (C_3), 119.6 (C_7), 115.2 (C_{3a}), 93.6 (C_5), 93.0 (C_6), 92.3 (C_7), 89.8 (C_4), 42.9 (C_1), 17.0 (C_8). Anal. Calcd for $\text{C}_{13}\text{H}_{10}\text{CrO}_3$: C, 58.65; H, 3.79. Found: C, 58.71; H, 3.88.

Synthesis of $[\eta^6\text{-2-Indenyl}]_2\text{benzene}]_2\text{tricarboxylchromium}$ (15**).** 2-Phenylindene (96 mg, 0.5 mmol) was heated with $\text{Cr}(\text{CO})_6$ (110 mg, 0.5 mmol) in dioxane (2.5 mL) at 125 °C in a sealed tube for 2 days. The products were not separable chromatographically, but slow crystallization from ethyl acetate gave **14** and an X-ray quality sample of **15** (21 mg, 13%). Data for **15** are as follows. MS (ES) (m/z): [$\text{M} - \text{H}$] 327.06, 100%. ^1H NMR (400 MHz, CDCl_3 , numbering in accord with Figure 2): δ 7.53 (1H, d, $J = 7$ Hz, H_4), 7.46 (1H, d, $J = 7$ Hz, H_7), 7.38 (1H, t, $J = 7$ Hz, H_5), 7.23 (1H, t, $J = 7$ Hz, H_6), 7.16 (1H, s, H_3), 5.70 (2H, d, $J = 6$ Hz, $\text{H}_{9,13}$), 5.45 (2H, t, $J = 6$ Hz, $\text{H}_{10,12}$), 5.33 (1H, t, $J = 6$ Hz, H_{11}), 3.66 (2H, s, $\text{H}_{1,1'}$). ^{13}C NMR (100 MHz): δ 232.8 (Cr-CO's), 142.2 (C_2), 129.2 (C_3), 126.4 (C_4), 125.9 (C_6), 123.8 (C_7), 121.3 (C_5), 104.1 (C_8), 92.3 ($\text{C}_{10,12}$), 91.4 (C_{11}), 90.4 ($\text{C}_{9,13}$), 39.1 (C_1). Anal. Calcd for $\text{C}_{13}\text{H}_{10}\text{CrO}_3$: C, 65.86; H, 3.68. Found: C, 66.40; H, 3.98.

Preparation of $[\eta^5\text{-2-Phenylindenyl}]_2\text{tricarboxylrhenium}$ (16**).** 2-Phenylindene (96 mg, 0.5 mmol) was heated with $\text{Re}_2(\text{CO})_{10}$ (326 mg, 0.5 mmol) in decalin (2 mL) at 160 °C in a sealed tube for 2 days, and the products were separated chromatographically (eluent dichloromethane/cyclohexane) to give **16** (28 mg, 12%) as an off-white solid. Mp: 117 °C. ^1H NMR (400 MHz, CDCl_3 , numbering in accord with Figure 2): δ 7.54 (2H, m, $\text{H}_{4,7}$), 7.46 (2H, d, $J = 7$ Hz, $\text{H}_{9,13}$), 7.37 (2H, t, $J = 7$ Hz, $\text{H}_{10,12}$), 7.31 (1H, t, $J = 7$ Hz, H_{11}), 7.08 (2H, m, $\text{H}_{5,6}$), 6.16 (2H, s, $\text{H}_{1,3}$). ^{13}C NMR (100 MHz): δ 193.3 (Re-CO's), 132.0 (C_8), 129.1 (C_{11}), 128.8 ($\text{C}_{10,12}$), 126.7 ($\text{C}_{9,13}$), 123.5 (C_4), 126.2 ($\text{C}_{5,6}$), 113.8 (C_3), 107.6 ($\text{C}_{3a,7a}$), 69.9 ($\text{C}_{1,3}$). Anal. Calcd for $\text{C}_{18}\text{H}_{11}\text{ReO}_3$: C, 46.86; H, 2.40. Found: C, 46.70; H, 2.42.

Synthesis of $[\eta^5\text{-1-(2-Methylinden-3-yl)-2-methylindenyl}]_2\text{tricarboxylrhenium}$ (17**).** 2,2'-Dimethyl-1,1'-biindenyl (65 mg, 0.25 mmol) was heated with $\text{Re}_2(\text{CO})_{10}$ (160 mg, 0.25 mmol) in decalin (2 mL) at 160 °C in a sealed tube for 2 days, and the products were separated chromatographically (eluent ethyl dichloromethane/cyclohexane) to give a material containing **17** as the major component (36 mg, 27%). ^1H NMR (400 MHz, numbering in accord with Figure 3): δ 7.82 (1H, d, $J = 7$ Hz, H_{12}), 7.42 (1H, t, $J = 7$ Hz, H_{13}), 7.20 (1H, t, $J = 7$ Hz, H_{14}), 7.46 (1H, d, $J = 7$ Hz, H_{15}), 7.52 (1H, d, $J = 7$ Hz, H_4), 7.08 (1H, t, $J = 7$ Hz, H_5), 7.51 (1H, t, $J = 7$ Hz, H_6), 7.06 (1H, d, $J = 7$ Hz, H_7), 5.78 (1H, s, H_3), 3.67 and 3.58 (2H, each d, $J = 22$ Hz, $\text{H}_{9,9'}$), 2.43 (3H, s, H_{16}), 2.13 (3H, s, H_8). ^{13}C NMR (100 MHz, region 120–127 ppm unresolved): δ 193.9 (Re-CO's), 144.7 (C_{11a}), 144.3 (C_{10}), 141.0 (C_{15a}), 127.4 (C_{11}), 111.7 (C_2), 106.7 (C_7), 106.5 (C_{3a}), 85.7 (C_1), 70.4 (C_3), 44.4 (C_9), 15.8 (C_{16}), 13.2 (C_8). Anal. Calcd for $\text{C}_{23}\text{H}_{17}\text{ReO}_3$: C, 52.36; H, 3.25. Found: C, 52.50; H, 2.99.

Preparation of $[\eta^6\text{-}(9\text{-Anthracenyl})\text{benzene}]_2\text{tricarboxylchromium}$ (19**).** 9-Phenylanthracene (254 mg, 1 mmol) was heated with $\text{Cr}(\text{CO})_6$ (220 mg, 1 mmol) in the presence of a catalytic amount of Zn powder in dioxane (5 mL) at 125 °C (sealed tube) for 2 days, during which time formation of a deep purple solution was observed. After further heating for 1 day at 80 °C, the reaction mixture turned yellow and the products were separated chromatographically (eluent ethyl acetate/cyclohexane) to give **19** (27 mg, 7%) as a very bright yellow solid whose characteristics were consistent with the reported data.¹⁴ ^1H NMR (500 MHz, $\text{DMSO}-d_6$, numbering in accord with Figure 4): δ 9.30 (1H, d, $J = 8$ Hz, H_1), 8.77 (1H, s, H_{10}), 8.16 (2H, d, $J = 8$ Hz, $\text{H}_{4,5}$), 7.88 (1H, d, $J = 8$ Hz, H_8), 7.59 (2H, t, $J = 7$ Hz, $\text{H}_{3,6}$), 7.53 (1H, t, $J = 7$ Hz, $\text{H}_{2,7}$), 6.13 (2H, d, $J = 7$ Hz, $\text{H}_{12,16}$), 6.06 (1H, t, $J = 6$ Hz, H_{14}), 5.96 (2H, t, $J = 6$ Hz, $\text{H}_{13,15}$). ^{13}C NMR (125 MHz): δ 234.1 (Cr-CO's), 131.9 (C_{8a}), 131.2 ($\text{C}_{4a,10a}$), 129.7 (C_{10}), 129.4 ($\text{C}_{4,5}$), 128.8 (C_9), 128 (C_{9a}), 125.8 ($\text{C}_{2,3,6,7}$), 125.6 (C_8), 125.5 (C_1), 110.0 (C_{11}), 101.2 ($\text{C}_{12,16}$), 93.7 ($\text{C}_{13,15}$), 96.6 (C_{14}).

Synthesis of $[\eta^5\text{-2-(9-Anthracenyl)indenyl}]_2\text{tricarboxylrhenium}$ (20**).** 2-(9-Anthracenyl)indene (**3a**; 116 mg, 0.4 mmol) was heated with $\text{Re}_2(\text{CO})_{10}$ (326 mg, 0.5 mmol) in decalin (2 mL) at 160 °C in a sealed tube for 2 days, and the products were separated chromatographically (eluent dichloromethane/cyclohexane) to give **20** (50 mg, 22%) as a yellow solid. Mp: 180 °C. ^1H NMR (500 MHz, CDCl_3 , numbering in accord with Figure 5): δ 8.60 (2H, d, $J = 9$ Hz, $\text{H}_{1,8}$), 8.51 (1H, s, H_{10}), 8.00 (2H, d, $J = 8$ Hz, $\text{H}_{4,5}$), 7.66 (2H, m, $\text{H}_{13,16}$), 7.53 (2H, t, $J = 7$ Hz, $\text{H}_{2,7}$), 7.47 (2H, t, $J = 7$ Hz, $\text{H}_{3,6}$), 7.18 (2H, m, $\text{H}_{14,15}$), 6.35 (2H, s, $\text{H}_{12,17}$). ^{13}C NMR (125 MHz): δ 193.3 (Re-CO's), 131.3 ($\text{C}_{4a,8b}$), 130.3 ($\text{C}_{4b,8a}$), 129.8 (C_{10}), 129.0 ($\text{C}_{4,5}$), 126.9 (C_9), 126.5 ($\text{C}_{14,15}$), 126.1 ($\text{C}_{2,7}$), 126.0 ($\text{C}_{1,8}$), 125.0 ($\text{C}_{3,6}$), 123.8 ($\text{C}_{13,16}$), 112.6 (C_{11}), 106.6 ($\text{C}_{12a,16a}$), 77.5 ($\text{C}_{12,17}$). Anal. Calcd for $\text{C}_{26}\text{H}_{15}\text{ReO}_3$: C, 55.60; H, 2.69. Found: C, 55.8; H, 2.95.

Synthesis of $[\eta^6\text{-2-(9-Anthracenyl)indene}]_2\text{tricarboxylchromium}$ (21**).** 2-(9-Anthracenyl)indene (**3a**; 116 mg, 0.4 mmol) was heated with $\text{Cr}(\text{CO})_6$ (110 mg, 0.5 mmol) in dioxane (2 mL) at 125 °C in a sealed tube for 2 days, and the products were separated chromatographically (eluent ethyl acetate/cyclohexane) to give **21** (72 mg, 42%) as a yellow solid. ^1H NMR (500 MHz, $\text{DMSO}-d_6$, numbering in accord with Figure 5): δ 8.66 (1H, s, H_{10}), 8.13 (2H, d, $J = 6.4$ Hz, $\text{H}_{4,5}$), 7.94 (2H, d, $J = 7$ Hz, $\text{H}_{1,8}$), 7.54 (2H, t, $J = 7$ Hz, $\text{H}_{3,6}$), 7.47 (2H, t, $J = 7$ Hz, $\text{H}_{2,7}$), 6.41 (2H, d, $J = 7$ Hz, $\text{H}_{13,16}$), 5.79 (2H, t, $J = 7$ Hz, $\text{H}_{14,15}$), 6.95 (1H, s, H_{17}), 4.17 and 3.87 (2H, both d, $J = 22$ Hz, $\text{H}_{12,12'}$). ^{13}C NMR (125 MHz): δ 235.5 (Cr-CO's), 149.0 (C_{11}), 131.5 (C_{17}), 131.2 ($\text{C}_{4a,8b}$), 131.1 (C_9), 129.7 ($\text{C}_{4b,8a}$), 129.0 ($\text{C}_{4,5}$), 127.6 (C_{10}), 126.4 ($\text{C}_{2,7}$), 126.0 ($\text{C}_{1,8}$), 126.0 ($\text{C}_{3,6}$), 117.5 (C_{16a}), 115.9 (C_{12a}), 93.8 ($\text{C}_{14,15}$), 93.2 (C_{16}), 91.5 (C_{13}), 44.8 (C_{12}). Anal. Calcd for $\text{C}_{26}\text{H}_{16}\text{CrO}_3$: C, 72.89; H, 3.76. Found: C, 72.66; H, 4.00.

Synthesis of $[\eta^5\text{-3-(9-Anthracenyl)indenyl}]_2\text{tricarboxylrhenium}$ (23**).** 3-(9-Anthracenyl)indene (**3b**; 116 mg, 0.4 mmol) was heated with $\text{Re}_2(\text{CO})_{10}$ (130 mg, 0.2 mmol) in decalin (2 mL) at 180 °C in a sealed tube for 2 days, and the products were separated chromatographically (eluent dichloromethane/cyclohexane) to give **23** (27 mg, 12%) as a yellow solid. Mp: 165 °C. ^1H NMR (600 MHz, CDCl_3 , numbering in accord with Figure 8): δ 9.42 (1H, d, $J = 9$ Hz, H_1), 8.60 (1H, s, H_{10}), 8.10 (1H, d, $J = 8$ Hz, H_4), 8.03 (1H, d, $J = 8$ Hz, H_5), 7.68 (1H, t, $J = 9$ Hz, H_2), 7.67 (1H, d, $J = 9$ Hz, H_{12}), 7.55 (1H, t, $J = 7$ Hz, H_3), 7.42 (1H, m, H_6), 7.25 (2H, m, $\text{H}_{7,8}$), 7.12 (1H, m, H_{13}), 7.01 (2H, m, $\text{H}_{14,15}$), 6.12 (1H, d, $J = 2.7$ Hz, H_{16}), 5.99 (1H, d, $J = 2.7$ Hz, H_{17}). ^{13}C NMR (150 MHz): δ 197.2 (Re-CO's), 131.9 (C_{8a}), 131.4 (C_{4b}), 131.2 (C_{4a}), 129.3 (C_{8b}), 129.2 (C_{10}), 128.9 ($\text{C}_{4,5}$), 126.8 (C_1), 126.7 (C_{14}), 126.6 (C_8), 126.1 (C_7), 125.7 (C_{13}), 125.5 (C_2), 125.4 (C_3), 124.9 (C_{12}), 124.5 (C_9), 124.3 (C_6), 122.7 (C_{15}), 111.3 (C_{15a}), 105.1 (C_{11}), 95.2 (C_{17}), 90.5 (C_{11a}), 71.6 (C_1). Anal. Calcd for $\text{C}_{26}\text{H}_{15}\text{ReO}_3$: C, 55.60; H, 2.69. Found: C, 55.35; H, 3.00.

Synthesis of $[\eta^6\text{-3-(9-Anthracenyl)indene}]_2\text{tricarboxylchromium}$ (24**).** 3-(9-Anthracenyl)indene (**3b**; 116 mg, 0.4 mmol) was heated with $\text{Cr}(\text{CO})_6$ (110 mg, 0.5 mmol) in dioxane (2 mL) at 125 °C in a sealed tube for 2 days, and the products were separated chromatographically (eluent ethyl acetate/cyclohexane) to give **23** (98 mg, 57%) as a yellow solid. ^1H NMR (600 MHz, $\text{DMSO}-d_6$,

Table 2. Crystallographic Data for 13, 15–17, 20, and 21

	13	15	16	17	20	21
formula	C ₁₃ H ₁₀ O ₃ Cr	C ₁₈ H ₁₂ O ₃ Cr	C ₁₈ H ₁₁ O ₃ Re	C ₂₃ H ₁₇ O ₃ Re	C ₂₆ H ₁₅ O ₃ Re	C ₂₆ H ₁₆ O ₃ Cr
<i>M_r</i>	266.21	328.28	461.47	527.57	561.58	428.39
cryst syst	orthorhombic	monoclinic	orthorhombic	monoclinic	monoclinic	monoclinic
space group (No.)	<i>Pnma</i> (62)	<i>P2₁/n</i> (14)	<i>P2₁2₁2₁</i> (19)	<i>P2₁/c</i> (14)	<i>P2₁/c</i> (14)	<i>P2₁/c</i> (14)
<i>a</i> (Å)	15.649(2)	11.3264 (15)	8.3815(4)	15.186(3)	8.0644(9)	12.9308(17)
<i>b</i> (Å)	10.3612(15)	10.9998(15)	10.1729(4)	8.2628(15)	24.041(3)	11.2668(15)
<i>c</i> (Å)	6.9097(10)	12.2185(16)	52.705(2)	16.016(3)	10.9718(12)	12.9929(17)
α (deg)	90	90	90	90	90	90
β (deg)	90	112.510(2)	90	111.483(3)	109.801(3)	98.190(4)
γ (deg)	90	90	90	90	90	90
<i>V</i> (Å ³)	1115.5(3)	1406.3(3)	4493.8(3)	1870.0(6)	2001.4(4)	1873.6(4)
<i>Z</i>	4	4	12	4	4	4
σ_{calcd} (g cm ⁻³)	1.585	1.550	2.046	1.874	1.864	1.519
<i>T</i> (K)	100(2)	100(2)	100(2)	100(2)	100(2)	100(2)
μ (mm ⁻¹)	1.016	0.823	8.121	6.518	6.097	0.638
<i>F</i> (000)	544	672	2616	1016	1080	880
θ range (deg)	2.60–28.79	2.09–28.27	0.77–30.57	2.58–28.29	1.69–26.45	1.59–24.97
index ranges	–20 ≤ <i>h</i> ≤ 21 –13 ≤ <i>k</i> ≤ 13 –9 ≤ <i>l</i> ≤ 9	–15 ≤ <i>h</i> ≤ 15 –14 ≤ <i>k</i> ≤ 14 –16 ≤ <i>l</i> ≤ 16	–8 ≤ <i>h</i> ≤ 11 –14 ≤ <i>k</i> ≤ 13 –74 ≤ <i>l</i> ≤ 73	–20 ≤ <i>h</i> ≤ 20 –11 ≤ <i>k</i> ≤ 11 –21 ≤ <i>l</i> ≤ 21	–10 ≤ <i>h</i> ≤ 10 –30 ≤ <i>k</i> ≤ 29 –13 ≤ <i>l</i> ≤ 13	–15 ≤ <i>h</i> ≤ 15 –13 ≤ <i>k</i> ≤ 13 –15 ≤ <i>l</i> ≤ 15
no. of rflns measd	9827	13 882	51 259	18 324	17 722	14 351
no. of indep rflns	1466	3460	13 490	4613	4113	3281
no. of data/restraints/params	1466/0/86	3460/0/247	13 490/291/596 ^a	4613/0/246	4113/0/271	3281/0/271
final <i>R</i> values (<i>I</i> > 2σ(<i>I</i>))						
<i>R</i> 1	0.0386	0.0358	0.0474	0.0287	0.0311	0.0540
<i>wR</i> 2	0.1005	0.0926	0.0950	0.0645	0.0703	0.1213
<i>R</i> values (all data)						
<i>R</i> 1	0.0425	0.0415	0.0487	0.0346	0.0381	0.0638
<i>wR</i> 2	0.1021	0.0959	0.0955	0.0667	0.0728	0.1252
GOF on <i>F</i> ²	1.196	1.056	1.283	1.048	1.067	1.129

^aDELU (rigid bond) restraints applied to all thermal displacement parameters.

d_o, numbering in accord with Figure 8): δ 8.71 (1H, s, H₁₀), 8.18 (1H, d, *J* = 9 Hz, H₃), 8.16 (1H, d, *J* = 9 Hz, H₄), 8.13 (1H, d, *J* = 9 Hz, H₁), 7.67 (1H, d, *J* = 9 Hz, H₈), 7.56 (1H, t, *J* = 7 Hz, H₆), 7.55 (1H, t, *J* = 7 Hz, H₃), 7.50 (1H, t, *J* = 7 Hz, H₂), 7.47 (1H, t, *J* = 7 Hz, H₇), 6.89 (1H, s, H₁₇), 6.30 (1H, d, *J* = 6 Hz, H₁₅), 5.90 (1H, t, *J* = 6 Hz, H₁₄), 5.31 (1H, d, *J* = 6 Hz, H₁₂), 5.29 (1H, t, *J* = 6 Hz, H₁₃), 4.15 and 3.87 (2H, each d, *J* = 24 Hz, H_{16,16'}). ¹³C NMR (150 MHz): δ 234.4 (Cr-CO's), 139.2 (C₁₇), 138.7 (C₁₁), 129.7 (C_{8a}), 131.6 (C_{4a}), 131.3 (C_{8b}), 130.4 (C_{4b}), 129.3 (C₅), 128.0 (C₁₀), 127.9 (C₉), 126.9 (C₄), 126.8 (C₇), 126.6 (C₁), 126.4 (C₂), 126.1 (C₃), 126.0 (C_{6,8}), 118.4 (C_{15a}), 117.5 (C_{11a}), 96.3 (C₁₄), 90.6 (C₁₃), 92.5 (C₁₂), 90.4 (C₁₅), 39.6 (C₁₆). Anal. Calcd for C₂₆H₁₆CrO₃: C, 72.89; H, 3.76. Found: C, 72.23; H, 3.96.

Synthesis of [η^6 -1,4-Diphenylbicyclo[2.2.2]octane)-tricarboxylchromium (26). 1,4-Diphenylbicyclo[2.2.2]octane (131 mg, 0.5 mmol) was heated with Cr(CO)₆ (110 mg, 0.5 mmol) in dioxane (2 mL) at 125 °C in a sealed tube for 2 days, and the products were separated chromatographically (eluent ethyl acetate/cyclohexane) to give 26 (178 mg, 45%) as a yellow solid. ¹H NMR (500 MHz, CD₂Cl₂, numbering in accord with Figure 11): δ 7.36 (2H, d, *J* = 8 Hz, H_{16,20}), 7.31 (2H, t, *J* = 7 Hz, H_{17,19}), 7.19 (1H, t, *J* = 7 Hz, H₁₈), 5.49 (2H, d, *J* = 7 Hz, H_{10,14}), 5.39 (1H, t, *J* = 7 Hz, H₁₂), 5.18 (2H, t, *J* = 7 Hz, H_{11,13}), 1.96 (6H, m, H_{2,6,7}), 1.90 (6H, m, H_{3,5,8}). ¹³C NMR (125 MHz): δ 233.6 (Cr-CO's), 148.9 (C₁₅), 128.2 (C_{17,19}), 125.4 (C_{16,20}), 125.8 (C₁₈), 121.0 (C₉), 93.9 (C₁₂), 93.0 (C_{10,14}), 90.4 (C_{11,13}), 34.9 (C₄), 34.4 (C₁), 32.8 (C_{3,5,8}), 32.4 (C_{2,6,7}). Anal. Calcd for C₂₃H₂₂CrO₃: C, 69.34; H, 5.57. Found: C, 69.57; H, 5.60.

Preparation of [η^6 -(9-Phenyl)-1,2,3,4,4a,9a-triptycene]-tricarboxylchromium (28). 9-Phenyltriptycene (100 mg, 0.3 mmol) was heated with Cr(CO)₆ (110 mg, 0.5 mmol) in dioxane (2 mL) at 125 °C in a sealed tube for 2 days, and the products were

separated chromatographically (eluent ethyl acetate/cyclohexane) to give 28 (60 mg, 43%) as a yellow solid. ¹H NMR (500 MHz, CDCl₃, numbering in accord with Figure 12): δ 8.12 (2H, d, *J* = 8 Hz, H_{18,22}), 7.80 (1H, m, H₈), 7.67 (2H, t, *J* = 8 Hz, H_{19,21}), 7.56 (1H, t, *J* = 8 Hz, H₂₀), 7.45 (1H, d, *J* = 7 Hz, H₁₆), 7.40 (1H, m, H₅), 7.15 (1H, t, *J* = 7 Hz, H₁₅), 7.02 (2H, m, H_{6,7}), 7.00 (1H, t, *J* = 7 Hz, H₁₄), 6.85 (1H, d, *J* = 7 Hz, H₁₃), 5.70 (2H, d, *J* = 6 Hz, H₄), 5.40 (1H, d, *J* = 6 Hz, H₁), 5.18 (1H, t, *J* = 6 Hz, H₃), 5.10 (1H, s, H₁₀), 5.05 (1H, t, *J* = 6 Hz, H₂). ¹³C NMR (125 MHz): δ 232.0 (Cr-CO's), 145.6 (C₁₂), 143.5 (C₁₁), 145.0 (C_{8a}), 146.5 (C_{8b}), 134.0 (C₁₇), 131.0 (C_{18,22}), 128.8 (C_{19,21}), 128.0 (C₂₀), 126.2 (C₁₅), 125.8 (C₆), 125.6 (C₁₄), 125.4 (C₇), 124.8 (C₈), 124.3 (C₅), 124.2 (C₁₃), 123.2 (C₁₆), 120.0 (C_{4a}), 119.0 (C_{4b}), 92.0 (C₁), 90.6 (C₄), 89.8 (C₂), 89.0 (C₃), 58.5 (C₉), 53.0 (C₁₀). Anal. Calcd for C₂₃H₂₂CrO₃: C, 74.67; H, 3.89. Found: C, 74.82; H, 4.10.

Synthesis of [η^5 -3-(9-Triptycyl)indenyl]tricarboxylrhenium (33). 9-(3-Indenyl)triptycene (123 mg, 0.3 mmol) was heated with Re₂(CO)₁₀ (130 mg, 0.2 mmol) in decalin (2 mL) at 180 °C in a sealed tube for 2 days, and the products were separated chromatographically (eluent dichloromethane/cyclohexane) to give 33 (14 mg, 7%) as a yellow solid. Mp: 182 °C. ¹H NMR (500 MHz, C₂D₂Cl₄, numbering in accord with Figure 13): δ 8.15 (1H, d, *J* = 8 Hz, H₁), 7.77 (1H, d, *J* = 7 Hz, H₈), 7.69 (1H, d, *J* = 9 Hz, H₂₀), 7.48 (2H, d, *J* = 7 Hz, H_{4,16}), 7.45 (1H, m, H₅), 7.27 (1H, d, *J* = 9 Hz, H₂₃), 7.16 (2H, t, *J* = 7 Hz, H₂ and H₂₁), 7.10 (2H, t, *J* = 7 Hz, H₃ and H₇), 7.05 (2H, m, H₆ and H₂₂), 7.04 (1H, m, H₁₅), 6.76 (1H, t, *J* = 7 Hz, H₁₄), 6.31 (1H, s, H₁₈), 6.26 (1H, s, H₁₉), 5.85 (1H, d, *J* = 7 Hz, H₁₃), 5.46 (1H, s, H₁₀); ¹³C NMR (125 MHz): δ 193.0 (Re-CO's), 147.4 (C_{8b}), 147.2 (C_{4a}), 146.1 (C₁₂), 145.2 (C_{8a}), 144.6 (C₁₁), 143.1 (C_{4b}), 127.7 (C₂₂), 125.2 (C₂₃), 126.4 (C₂₁), 124.7 (C₂₀), 126.4 (C₁₅), 125.5 (C₆), 126.2 (C₁₄), 124.2 (C₇), 124.6 (C₈), 123.6 (C₅), 123.8 (C₁₃), 126.6

Table 3. Crystallographic Data for 23, 24, 26, 28, and 33

	23	24	26	28	33
formula	C ₂₆ H ₁₃ O ₃ Re	C ₂₆ H ₁₆ O ₃ Cr	C ₂₃ H ₂₂ O ₃ Cr	C ₂₉ H ₁₈ O ₃ Cr	C ₃₂ H ₁₉ O ₃ Re•0.805(C ₆ H ₁₂)•0.195(CHCl ₃)
M _r	561.58	428.39	398.41	466.43	728.59
cryst syst	triclinic	monoclinic	monoclinic	monoclinic	triclinic
space group (No.)	P $\bar{1}$ (2)	C2/c (15)	P2 ₁ /n (14)	P2 ₁ /c (14)	P $\bar{1}$ (2)
a (Å)	7.7534(7)	22.3421(19)	6.0013(4)	13.6588(14)	10.2673(8)
b (Å)	9.9783(9)	10.7303(9)	19.5708(12)	14.8955(15)	11.5569(9)
c (Å)	12.5568(12)	18.7235(15)	15.5061(9)	11.3118(11)	13.1236(10)
α (deg)	85.996(2)	90	90	90	88.489(1)
β (deg)	85.794(2)	116.783(2)	98.909(1)	113.353(2)	77.448(1)
γ (deg)	78.929(2)	90	90	90	70.282(1)
V (Å ³)	949.28(15)	4007.2(6)	1799.22(19)	2112.9(4)	1429.01(19)
Z	2	8	4	4	2
σ_{calcd} (g cm ⁻³)	1.965	1.420	1.471	1.466	1.693
T (K)	100(2)	293(2)	100(2)	100(2)	100(2)
μ (mm ⁻¹)	6.427	0.596	0.657	0.572	4.336
F(000)	540	1760	832	960	720.1
θ range (deg)	2.08–30.68	2.04–21.58	1.69–31.55	2.12–26.58	2.16–32.04
index ranges	–11 ≤ h ≤ 11 –14 ≤ k ≤ 14 –17 ≤ l ≤ 17	–23 ≤ h ≤ 22 –11 ≤ k ≤ 11 –19 ≤ l ≤ 19	–8 ≤ h ≤ 8 –27 ≤ k ≤ 27 –22 ≤ l ≤ 22	–17 ≤ h ≤ 17 –18 ≤ k ≤ 18 –14 ≤ l ≤ 14	–15 ≤ h ≤ 15 –16 ≤ k ≤ 16 –19 ≤ l ≤ 18
no. of rflns measd	22 282	9873	20 902	18 597	34 578
no. of indep rflns	5765	2308	5637	4399	9245
no. of data/restraints/params	5765/0/271	2308/131/271 ^a	5637/0/332	4399/18/370	9245/31/414
final R values (I > 2σ(I))					
R1	0.0294	0.0431	0.0357	0.0566	0.0255
wR2	0.0644	0.1124	0.0934	0.1461	0.0634
R values (all data)					
R1	0.0348	0.0508	0.0409	0.0634	0.0274
wR2	0.0664	0.1184	0.0964	0.1510	0.0641
GOF on F ²	1.048	1.069	1.062	1.072	1.085

^aDELU (rigid bond) restraints applied to all thermal displacement parameters.

(C₁₆), 124.1 (C₁), 124.4 (C₄), 123.7 (C₂), 125.6 (C₃), 111.5 (C_{23a}), 105.7 (C_{19a}), 95.1 (C₁₈), 87.9 (C₁₇), 74.3 (C₁₉), 55.7 (C₉), 54.9 (C₁₀). Anal. Calcd for C₃₂H₁₉ReO₃•C₆H₁₂: C, 63.23; H, 4.33. Found: C, 63.14; H, 4.54.

Quantum Chemistry Calculations. These calculations were performed using the SPARTAN 08 package on a Pentium PC. Calculations of molecular geometries under vacuum were done at the DFT B3LYP level using the 6-31G* basis set, as exemplified in the Supporting Information. For rhenium complexes, the corresponding manganese analogues were used as appropriate models.

X-ray Measurements for 13, 15–17, 20, 21, 23, 24, 26, 28, and 33. Crystal data were collected using a Bruker SMART APEX CCD area detector diffractometer. A full sphere of reciprocal space was scanned by ψ - ω scans. Pseudoempirical absorption correction based on redundant reflections was performed by the program SADABS.²⁵ The structures were solved by direct methods using SHELXS-97²⁶ and refined by full-matrix least squares on F² for all data using SHELXL-97.²⁶ Hydrogen atom treatment varied from compound to compound, depending on the crystal quality. In 15, 26, and 28 all hydrogen atoms were located in the difference Fourier map and allowed to refine freely. In all other compounds hydrogen atoms were added at calculated positions and refined using a riding model. Their isotropic temperature factors were fixed to 1.2 times the equivalent isotropic displacement parameters of the parent atom. CCDC 880504 (13), 880495 (15), 880496 (16), 880498 (17), 880502 (20), 880503 (21), 880501 (23), 880499 (24), 880497 (26), 880500 (28), and 880505 (33) contain supplementary X-ray crystallographic data for this paper. These data can be obtained free of charge from the Cambridge Crystallographic Data Centre via http://www.ccdc.cam.ac.uk/data_request/cif. Crystallographic data for 13, 15–17, 20, and 21 are given in Table 2 and for 23, 24, 26, 28, and 33 in Table 3.

■ ASSOCIATED CONTENT

● Supporting Information

Figures and tables giving characterization data and additional details of the calculations and CIF files giving crystal data for 13, 15–17, 20, 21, 23, 24, 26, 28, and 33. This material is available free of charge via the Internet at <http://pubs.acs.org>.

■ AUTHOR INFORMATION

Corresponding Author

*E-mail: kirill.nikitin@ucd.ie (K.N.); michael.mcglinchey@ucd.ie (M.J.M.).

Notes

The authors declare no competing financial interest.

■ ACKNOWLEDGMENTS

We thank Science Foundation Ireland, University College Dublin, and the Centre for Synthesis and Chemical Biology funded by the Higher Education Authority's Programme for Research in Third-Level Institutions (PRTL) for generous financial support and the three reviewers for their perceptive and helpful comments.

■ REFERENCES

- (1) (a) This classification, of course, disregards whether the movement is cyclical, random, or directional and whether it is downhill or uphill energetically. Excellent analyses are found in: (a) Kay, E. R.; Leigh, D. A.; Zerbetto, F. *Angew. Chem., Int. Ed.* **2007**,

46, 72–191. (b) Balzani, V.; Credi, A.; Venturi, M. *Molecular Devices and Machines*, 2nd ed.; VCH: Weinheim, Germany, 2008.

(2) (a) Bissell, R. A.; Cordova, E.; Kaifer, A. E.; Stoddart, J. F. *Nature* **1994**, *369*, 133–137. (b) Nygaard, S.; Leung, K. C.-F.; Aprahamian, I.; Ikeda, T.; Saha, S.; Laursen, B. W.; Kim, S.-Y.; Hansen, S. W.; Stein, P. C.; Flood, A. H.; Stoddart, J. F.; Jeppesen, J. O. *J. Am. Chem. Soc.* **2007**, *129*, 960–970. (c) Nikitin, K.; Stolarczyk, J. K.; Lestini, E.; Fitzmaurice, D. *Chem. Eur. J.* **2008**, *14*, 1117–1128. (d) Saha, S.; Stoddart, J. F. *Chem. Soc. Rev.* **2007**, *36*, 77–92. (e) Balzani, V.; Clemente-León, M.; Credi, A.; Ferrer, B.; Venturi, M.; Flood, A. H.; Stoddart, J. F. *Proc. Nat. Acad. Sci.* **2006**, *103*, 1178–1183. (f) Altobello, S.; Nikitin, K.; Stolarczyk, J. K.; Lestini, E.; Fitzmaurice, D. *Chem. Eur. J.* **2008**, *14*, 1107–1116. (g) Murakami, H.; Kawabuchi, A.; Matsumoto, R.; Ido, T.; Nakashima, N. *J. Am. Chem. Soc.* **2005**, *127*, 15891–15899. (h) Abraham, W.; Grubert, L.; Grummt, U. W.; Buck, K. *Chem. Eur. J.* **2004**, *10*, 3562–3568. (i) Berna, J.; Leigh, D. A.; Lubomska, M.; Mendoza, S. M.; Perez, E. M.; Rudolf, P.; Teobaldi, G.; Zerbetto, F. *Nat. Mater.* **2005**, *4*, 704–710. (j) Jun, S. I.; Lee, J. W.; Sakamoto, S.; Yamaguchi, K.; Kim, K. *Tetrahedron Lett.* **2000**, *41*, 471–475. (k) Murakami, H.; Kawabuchi, A.; Kotoo, K.; Kunitake, M.; Nakashima, N. *J. Am. Chem. Soc.* **1997**, *119*, 7605–7606. (l) Raiteri, P.; Bussi, G.; Cucinotta, C. S.; Credi, A.; Stoddart, J. F.; Parrinello, M. *Angew. Chem., Int. Ed.* **2008**, *47*, 3536–3539. (m) Fioravanti, G.; Haraszkiwicz, N.; Kay, E. R.; Mendoza, S. M.; Bruno, C.; Marcaccio, M.; Wiering, P. G.; Paolucci, F.; Rudolf, P.; Brouwer, A. M.; Leigh, D. A. *J. Am. Chem. Soc.* **2008**, *130*, 2593–2601.

(3) (a) Nakamura, M.; Oki, M. *Bull. Chem. Soc. Jpn.* **1975**, *48*, 2106–2111. (b) Oki, M.; Fujino, I.; Kawaguchi, D.; Chuda, K.; Moritaka, Y.; Yamamoto, Y.; Tsuda, S.; Akinaga, T.; Aki, M.; Kojima, H.; Morita, N.; Sakurai, M.; Toyota, S.; Tanaka, Y.; Tanuma, T.; Yamamoto, G. *Bull. Chem. Soc. Jpn.* **1997**, *70*, 457–469. (c) Yamamoto, G.; Suzuki, M.; Oki, M. *Angew. Chem., Int. Ed. Engl.* **1981**, *20*, 607–608. (d) Zehm, D.; Fudickar, W.; Hans, M.; Schilde, U.; Kelling, A.; Linker, T. *Chem. Eur. J.* **2008**, *14*, 11429–11441. (e) Kelly, T. R.; Bowyer, M. C.; Bhaskar, K. V.; Bebbington, D.; Garcia, A.; Lang, F. R.; Kim, M. H.; Jette, M. P. *J. Am. Chem. Soc.* **1994**, *116*, 3657–3658. (f) Kelly, T. R.; Sestelo, J. P.; Tellitu, I. N. *J. Org. Chem.* **1998**, *63*, 3655–3665. (g) Kelly, T. R. *Acc. Chem. Res.* **2001**, *34*, 514–522. (h) Mazzanti, A.; Lunazzi, L.; Minzoni, M.; Anderson, J. E. *J. Org. Chem.* **2006**, *71*, 5474–5481. (i) Bott, G.; Field, L. D.; Sternhell, S. *J. Am. Chem. Soc.* **1980**, *102*, 5618–5626. (j) Llunell, M.; Alemany, P.; Bofill, J. M. *ChemPhysChem* **2008**, *9*, 1117–1119. (k) Carella, A.; Launay, J.-P.; Poteau, R.; Rapenne, G. *Chem. Eur. J.* **2008**, *14*, 8147–8156. (l) Durola, F.; Sauvage, J.-P.; Wenger, O. S. *Coord. Chem. Rev.* **2010**, *254*, 1748–1759. (m) Sauvage, J.-P. *Acc. Chem. Res.* **1998**, *31*, 611–619. (n) Bringmann, G.; Mortimer, A. J. P.; Keller, P. A.; Gresser, M. J.; Garner, J.; Breuning, M. *Angew. Chem., Int. Ed.* **2005**, *44*, 5384–5427.

(4) Nikitin, K.; Müller-Bunz, H.; Ortin, Y.; McGlinchey, M. J. *Chem. Eur. J.* **2009**, *15*, 1836–1843.

(5) (a) Harrington, L. E.; Cahill, L. S.; McGlinchey, M. J. *Organometallics* **2004**, *23*, 2884–2891. (b) Nikitin, K.; Müller-Bunz, H.; Ortin, Y.; McGlinchey, M. J. *Org. Biomol. Chem.* **2007**, *5*, 1952–1960. (c) Nikitin, K.; Müller-Bunz, H.; Ortin, Y.; Risse, W.; McGlinchey, M. J. *Eur. J. Org. Chem.* **2008**, 3079–3084. (d) Nikitin, K.; Fleming, C.; Müller-Bunz, H.; Ortin, Y.; McGlinchey, M. J. *Eur. J. Org. Chem.* **2010**, 5203–5216. (e) Nikitin, K.; Müller-Bunz, H.; Ortin, Y.; Muldoon, J.; McGlinchey, M. J. *Org. Lett.* **2011**, *13*, 256–259.

(6) Nikitin, K.; Müller-Bunz, H.; Ortin, Y.; Muldoon, J.; McGlinchey, M. J. *J. Am. Chem. Soc.* **2010**, *132*, 17617–17622.

(7) Ortin, Y.; Seward, C. M.; McGlinchey, M. J. In *Comprehensive Organometallic Chemistry III*; Crabtree, R. H., Mingos, D. M. P., Eds.; Elsevier: Oxford, U.K., 2006; Vol. 5. Chapter 69, pp 239–240.

(8) Kamikawa, K.; Watanabe, T.; Uemura, M. *J. Org. Chem.* **1996**, *61*, 1375–1384.

(9) (a) Watanabe, T.; Shakadou, M.; Uemura, M. *Synlett* **2000**, 1141–1144. (b) Hata, T.; Koide, H.; Uemura, M. *Synlett* **2000**, 1145–1147.

(10) McGlinchey, M. J.; Burns, R. C.; Hofer, R.; Top, S.; Jaouen, G. *Organometallics* **1986**, *5*, 104–109.

(11) (a) Albright, T. A.; Hofmann, P.; Hoffmann, R.; Lilly, C. P.; Dobosh, P. A. *J. Am. Chem. Soc.* **1983**, *105*, 3396–3411. (b) Oprunenko, Y. F. *Russ. Chem. Rev.* **2000**, *69*, 683–704. (c) Brydges, S.; Reginato, N.; Cuffe, L. P.; Seward, C. M.; McGlinchey, M. J. *C. R. Chim.* **2005**, *8*, 1497–1505. (d) Brydges, S.; Harrington, L. E.; McGlinchey, M. J. *Coord. Chem. Rev.* **2002**, *233–234*, 75–105. (e) Kirillov, E.; Kahlal, S.; Roisnel, T.; Georgelin, T.; Saillard, J.-Y.; Carpentier, J.-F. *Organometallics* **2008**, *27*, 387–393. (f) Clarke, D. T.; Mlekuz, M.; Sayer, B. G.; McCarry, B. E.; McGlinchey, M. J. *Organometallics* **1987**, *6*, 2201–2207. (g) Salzer, A.; Täschler, C. J. *Organomet. Chem.* **1985**, *294*, 261–266. (h) Decken, A.; Britten, J. F.; McGlinchey, M. J. *J. Am. Chem. Soc.* **1993**, *115*, 7275–7284. (i) Amatore, C.; Ceccon, A.; Santi, S.; Verpeaux, J.-N. *Chem. Eur. J.* **1997**, *3*, 279–285.

(12) (a) Nori-shargh, D.; Asadzadeh, S.; Ghanizadeh, F.-R.; Deyhimi, F.; Amini, M. M.; Jameh-Bozorghi, S. *J. Mol. Struct. (THEOCHEM)*. **2005**, *717*, 41–51. (b) Nowak, W.; Wierzbowska, M. *J. Mol. Struct. (THEOCHEM)* **1996**, *368*, 223–234.

(13) (a) Toyota, S.; Okuhara, H.; Oki, M. *Organometallics* **1997**, *16*, 4012–4015. (b) Dyson, P. J.; Humphrey, D. G.; McGrady, J. E.; Mingos, D. M. P.; Wilson, D. J. *J. Chem. Soc., Dalton Trans.* **1995**, 4039–4043. (c) Arce, A. J.; Machado, R.; De Sanctis, Y.; Isea, R.; Atencio, R.; Deeming, A. J. *J. Organomet. Chem.* **1999**, *580*, 339–343. (d) Khayatpoor, R.; Shapley, J. R. *Organometallics* **2000**, *19*, 2382–2388. (e) Top, S.; Lehn, J.-S.; Morel, P.; Jaouen, G. *J. Organomet. Chem.* **1999**, *583*, 63–68.

(14) (a) Cunningham, S. D.; Ofele, K.; Willeford, B. R. *J. Am. Chem. Soc.* **1983**, *105*, 3724–3725. (b) Own, Z. Y.; Wang, S. M.; Chung, J. F.; Miller, D. W.; Fu, P. P. *Inorg. Chem.* **1993**, *32*, 152–159.

(15) (a) Pophristic, V.; Goodman, L. *Nature* **2001**, *411*, 565–568. (b) Oki, M. *Top. Stereochem.* **1983**, *14*, 1–81.

(16) Baur, W. H. *Acta Crystallogr.* **1992**, *B48*, 745–746.

(17) (a) Mlekuz, M.; Bougeard, P.; Sayer, B. G.; McGlinchey, M. J.; Rodger, C. A.; Churchill, M. R.; Ziller, J. W.; Kang, S.-K.; Albright, T. A. *Organometallics* **1986**, *5*, 1656–1663. (b) Wescott, M. A.; Kakkar, A. K.; Taylor, N. J.; Roe, D. C.; Marder, T. B. *Can. J. Chem.* **1999**, *77*, 205–215.

(18) Crystal data: formula $C_{23}H_{14}CrO_3$, $M_r = 390.34$, orthorhombic, cell parameters $a = 10.4506(2)$ Å, $b = 16.0839(3)$ Å, $c = 20.7142(3)$ Å, $\alpha = \beta = \gamma = 90^\circ$, $V = 3481.78(11)$ Å³, $Z = 8$, space group $Pbca$ (No. 61).

(19) Since the chromium group is η^6 bonded whether it is attached to either the anthracenyl unit (in **18**) or the phenyl fragment (in **19**), the Cr@Ph nomenclature is used to distinguish these isomers and similarly for Cr@Ph and Cr@tricyclic in molecules **27** and **28**.

(20) (a) Mailvaganam, B.; McCarry, B. E.; Sayer, B. G.; Perrier, R. E.; Faggiani, R.; McGlinchey, M. J. *J. Organomet. Chem.* **1987**, *335*, 213–227. (b) Maliszka, K. L.; Chao, L. C. F.; Britten, J. F.; Sayer, B. G.; Jaouen, G.; Top, S.; Decken, A.; McGlinchey, M. J. *Organometallics* **1993**, *12*, 2462–2471.

(21) (a) Jaouen, G.; Meyer, A. *J. Am. Chem. Soc.* **1975**, *97*, 4667–4672. (b) Uemura, M.; Nishimura, H.; Kamikawa, K.; Shiro, M. *Inorg. Chim. Acta* **1994**, *222*, 63–70. (c) Bringmann, G.; Göbel, L.; Peters, K.; Peters, E.-M.; von Schnering, H. G. *Inorg. Chim. Acta* **1994**, *222*, 255–260. (d) Top, S.; Jaouen, G.; Vessières, A.; Abjean, J.-P.; Davoust, D.; Rodger, C. A.; Sayer, B. G.; McGlinchey, M. J. *Organometallics* **1985**, *4*, 2143–2150.

(22) (a) Gupta, H. K.; Brydges, S.; McGlinchey, M. J. *Organometallics* **1999**, *18*, 115–122. (b) Harrington, L. E.; Britten, J. F.; McGlinchey, M. J. *Can. J. Chem.* **2003**, *81*, 1180–1186.

(23) Mailvaganam, B.; Sayer, B. G.; McGlinchey, M. J. *J. Organomet. Chem.* **1990**, *395*, 177–185.

(24) Gancarz, R. A.; Blount, J. F.; Mislow, K. *Organometallics* **1985**, *4*, 2028–2032.

(25) SADABS; Bruker AXS Inc., Madison, WI, 2001.

(26) Sheldrick, G. M. *Acta Crystallogr.* **2008**, *A64*, 112–122.